Tomomichi Kato

University of Tsukuba, Tsukuba, Ibaraki, Japan

Handling Topical Editor, Geoscientific Model Development (GMD)

Re: GMD-2018-41

Dear Dr. Kato,

Thanks so much for sending us two referees' assessment again on our resubmitted manuscript "Carbon-nitrogen coupling under three schemes of model representation: a traceability analysis" (No. GMD-2018-41). We appreciate the positive comments and further suggested amendments from the referees, which are very helpful to improve the paper. We have carefully studied the reviews, and revised our manuscript accordingly. As a consequence, our manuscript has been further improved.

We confirm that all authors have met the authorship criteria.

We also declare that the submitted work is our own and that copyright has not been breached in seeking its publication.

Here are our detailed responses to the reviews. Please note that the comments from the reviewers are in ***italics*** followed by our responses in **regular** text.

We hope you will find our revision satisfactory for publication in ***Geoscientific Model Development***.

Yours Sincerely,

Xuhui & Jianyang

Xuhui Zhou, Jianyang Xia

School of Ecological and Environmental Sciences, East China Normal University

500 Dongchuan Road, Shanghai 200062, China

Email: xhzhou@des.ecnu.edu.cn, jyxia@des.ecnu.edu.cn

Response letter to comments (gmd-2018-41)

Topical Editor Decision: Publish subject to minor revisions (review by editor)

Dr. Tomomichi Kato

I like to inform you that your paper is again subject to minor revision.
If you resubmit your article, please note that you carefully respond to all the comments one by one.

[**Response**] Thanks so much for your and the referees' assessments. We carefully revised the manuscript according to the referees' comments and suggestions and made necessary changes. Please see below for the detailed responses point by point. We hope you will find our revision satisfactory.

Will Wieder's comment (Referee #1)

I appreciate the revisions made to this manuscript. Two additional questions and several technical corrections arose after reading the text. I trust these can be addressed without too much trouble.

[**Response**] Thank so much for your positive comment. We carefully revised the whole manuscript according to your comments and suggestions. Please see responses below.

Why aren't denitrification, or gaseous losses shown in Fig 3 or discussed with leaching losses (e.g. line 475)? Thomas et al. 2013 found big difference in the denitrification rates simulated by CLM4 and OC-N, so I'd assume at steady state the models make very different projections?

[**Response**] Thanks for pointing out what we have neglected. Yes, the nitrogen gaseous losses showed large variation among three carbon-nitrogen schemes in our study. SM1, SM3 and SM2 had the smallest, biggest and moderate annual mean value (0.46, 0.77 and 1.39 g N m^{-2} yr^{-1}), respectively. The differences of nitrogen gaseous losses among three C-N coupling schemes mainly due to both the nitrogen balance requirement and dynamics of soil mineral nitrogen (Eq. 15).

We have added three new panels (Figs. 3f, 3m and 3t) in the Figure 3, and revised the method, result and discussion sections in the revised version accordingly.

I'm not sure I completely understand the explanation ~ lines 530 and 558. It's true, that CLM4.5 has fixed tissue stoichiometry, but it uses a dynamic C allocation scheme that should modify the C allocation to wood, stoichiometry, and MRT (at least in transient simulations)? This would also affect the allocation to wood vs. fine roots during spinup, with proportionally less wood C allocation associated with lower NPP? Are these nuances of C allocation from

SM2 & 3 brought into the TECO simulations presented? If not, maybe this is more of a nuance of how the sensitivities were calculated, but perhaps worth clarifying?

[**Response**] Sorry for the confusion. Yes, the nitrogen effects modify the C allocation (vector *B*) and thus the baseline C residence time (baseline MRT, Eq. 30, Fig 8a) for the SM2 (CLM4.5bgc), which further affect the mean ecosystem residence time (MRT). Based on our traceability analysis framework, we divided the nitrogen effects on MRT into two parts, one is from C allocation (vector *B* in Eq. 29 and Eq. 30) and the other is the N scalar on the *C* matrix (i.e., ξ_N in Eq. 31, we named it as in this study). We have discussed the N scalar (i.e., ξ_N) on Lines 551-569 in this study.

Technical corrections
L 85: should be 'dynamics'

[**Response**] Done as suggested.

L 103: I'm not really sure what "achieved predictive ability" means? Maybe delete this entire clause after the end of the parenthesis in line 102
[**Response**] Sorry for the confusion. As suggested, we deleted the "compared to the achieved predictive ability" in revised version.

L 109: are references needed for these models, as well as a description of their abbreviated names?

[**Response**] We have added the references and description of abbreviated names for each mode. The sentence was revised as "Three schemes of model representation were conducted mainly based on carbon-nitrogen coupling version of TECO (TECO-CN, Weng and Luo, 2008, [SM1]), Community Land Model Version 4.5 (CLM 4.5, Koven et al., 2013; Oleson et al., 2013, [SM2]) and carbon-nitrogen coupling version of the Organizing Carbon and Hydrology in Dynamic Ecosystems model (O-CN, Zaehle and Friend, 2010; Zaehle et al., 2011, [SM3]) (Table 1)."

L 153: it seems to introduce talk about "plant, litter and soil N pools" immediately following mention of the inorganic N pool. Consider revising "There are nine organic N pools - including plant, litter and soil N pools - and one inorganic soil N pool".

[**Response**] We revised the sentence as "There are nine organic N pools, including plant, litter and soil N pools, and one inorganic soil N pool"

Eq 20 & Line 463, Maybe worth citing Cleveland et al 1999, which is the source of this CLM4.5 approach for BNF (and I'm assuming for O-CN).

[**Response**] We added the reference in Line 481.

L 350, why not convert to mg N m^-2 d^-1 so the values are intelligible? Also, is the daily variation important here, or the total flux calculated by each model? My guess is both, but the latter is never really described (although it's displayed in the right column of Fig 3)?

[**Response**] Thanks for your comments and suggestions. The variation of N processes is mainly driven by the environment forcing, external N supply and ecosystem N demand. In this study, we can demonstrate the different effects on daily variations from the three C-N coupling representations.

We converted the units to mg N m^{-2} d^{-1} and added those description in this revised version.

L 353 & 354, no daily variation for leaching or N_{fix} is reported here?

[**Response**] Thanks for pointing out what we have neglected. The daily variations for leaching and biological nitrogen fixation were added in the revised version.

L 370 & Fig 4, how does one generate a positive NEE for all years in all model configurations if steady state conditions were achieved before starting the transient simulation? By definition, it seems NEE should be zero over the years correspond the equilibrium conditions? I don't understand how / or why a NSC pool would affect the calculation of NEE, is the model just storing up NSC?

[**Response**] Sorry for the confusion. The NSC pool is used to meet excess demand for maintenance respiration during periods with low photosynthesis (e.g. at night, during winter for perennial vegetation) in the TECO model. The initial value of NSC pool is set to eliminate running a deficit of NPP (negative state), while this effect does not include in calculating NEE in original version of TECO model. In this case, the total respiration is greater than the GPP for each year, thus generate a positive NEE. To eliminate confusion, we have recalculated the NEE, and revised the methods, results and discussion sections accordingly.

Fig 5, would it make more sense to plot both panels with a log y axis to show variation in bools and stoichiometry?

[**Response**] We have replotted Fig 5 with a log y axis as suggested.

Line 414 and 416, what to b2 and b3 refer to? Is this eq 2 & 3, if so maybe refer to these equations instead?

[**Response**] Sorry for the confusion. The b2 and b3 represent the coefficients of partitioning of NPP to wood and root. In order to eliminate confusion, we delete "(b2)" and "(b3)" in the Line 432 and 434.

L 452, isn't thus just Jmax in the Farquhar model (not Vjmax)?

[**Response**] Thanks for your correction. We replaced "Vjmax" with "Jmax" in the revised version.

L 538, is this more specifically related to vegetation C:N ratio (not total)

[**Response**] Done as suggested. We replaced the "total C:N ratio" to "vegetation C:N ratio" in the revised version.

(Anonymous Referee #2)

[General comments]

I appreciate the authors to respond to my comments to the previous manuscript. The revised manuscript has been much improved, but I think there still remains several points that should be clearer, including technical corrections.

[**Response**] Thank so much for your positive comment. We carefully revised the whole manuscript according to your comments and suggestions. Please see responses below.

- Eq (13): The numbers for pools (i=4~8) are defined in L296 and thus not yet defined here.

[**Response**] We added "where $CN0_i$ and CN_i ($i = 4, 5, 6, 7, 8$) are the C:N ratios of metabolic litter, structural litter, fast, slow and passive soil organic C pools at first- and current-time step, respectively." in the revised version.

- Eq (23): how did you get the parameter value for vmax? Nuptake in SM3 looks strongly dependent on the choice of this parameter, but not specified in the text.

[**Response**] For the O-CN model, the value of *vmax* is an empirical constant (Zaehle and Friend, 2010; Kronzucker et al., 1995, 1996), which set as 0.514. We added those information in this revised version.

In addition, in the third factor of "1/(Nmin x KNmin)", should "Nmin" be replaced by "SNmin"?

[**Response**] Yes, Thanks for your correction. We replaced the "*Nmin*" with "*SNmin*" in revised version.

- Eq (31): I apologize if I misunderstand, but it seems "Tau_E = Xi-1 Tau'_E" should be "Tau_E = Xi Tau'_E". Please check again.

[**Response**] Based on the Eq.28: $\frac{dX(t)}{dt} = BU(t) - A\xi CX(t)$, which makes left part equal to zero, the steady-state values of all carbon pools (X_{ss}) can be rearranged as:

$$X_{ss} = (A\xi C)^{-1}BU_{ss} = \xi C^{-1}A^{-1}BU_{ss} = \xi^{-1}C^{-1}A^{-1}BU_{ss} = \xi^{-1}\tau'_E U_{ss} = \tau_E U_{ss}$$

So, $\tau_E = \xi^{-1}\tau'_E$.

- Eq (34): CN_i^0 is defined here as the ratio at t=0, but defined in Eq (8) as that of last time step.

[**Response**] Thanks for pointing our mistake. We corrected the "last time step" to "first time step" in the revised version.

- *L341: In the sensitivity test, you increased/decreased 50% of each N-process. How did you make such changes in each process? For example, it is easy to change BNF by 50%, but I cannot imagine how you made the changes in the processes of PMC, PS, SS, etc. Readers will need brief explanations on this issue.*

[**Response**] Thanks for your comments and suggestions. To do sensitivity test, we 1) run the model to the steady state, 2) set the steady state as the initial state (C and N pool sizes) and make change (increased/decreased 50%) in one nitrogen process to run the model to steady state again, 3) calculate the relative changes of NPP, MRT and ecosystem C storage capacity between the two steady states using Eq 35, 36 and 37. We added those description in Lines 350-353.

- *Fig. 3o and 3q: In my understanding, since your analysis is based on steady-state simulations, the N budgets should be closed: BNF+Ndeposition should be comparable with the magnitude of Nleaching + Ngassing. However, in SM3, BNF looks much larger than Nleaching (and looks much smaller in SM1). 1000 years spin-up was not enough for the simulations? or other reasons? Do I miss something?*

[**Response**] Thanks for pointing out what we have neglected. Yes, for the TECO model in our study, $BNF+N_{deposition} \approx N_{leaching} + N_{gas\ losing}$. We added the results for nitrogen gaseous losses in the revised version, including three new panels (Figs. 3f, 3m and 3t) in the Figure 3, and revised the method, result and discussion sections accordingly.

- *L368-369, "SM1 and SM2 schemes increased ~~ 12% and 27%": maybe "SM1 and SM2" is "SM1 and SM3 ~~" .*

[**Response**] Thanks. We have corrected the "SM1 and SM2" to "SM1 and SM3" in the revised version.

- *L386, "Because of the hypothesis of Nuptake for free, SM2 had the highest CUE among three C-N schemes": This is slightly ambiguous for me. Does "Nuptake for free" mean "no C-cost on N uptake"?*

[**Response**] Yes, in the CLM4.5, plant uptake nitrogen from soil do not require the expenditure of energy in the form of carbon.

- *L446: Maybe "Our results showed … (Figs. 3a and 3g)" is "Our results showed …(Figs. 4a and 4g)"*

[**Response**] Corrected.

- *L473, "plant N uptake is enough for growth": maybe you forget "not".*

[**Response**] We added "not" in Lines 491

- *L483-L505: I'm still suffering from understanding the logical linking between the first half of this part (general understandings(?), L483-494) and the latter (claims obtained from your analysis(?), L494-505). For example, in the former part, you mention "the residence time of*

N in SOM appears to be an important factor", but such discussion on residence time does not appear in the latter part...

Or you may intend to discuss first the residence time effect on plant production and then the effect of stoichiometry. If so, you should discuss the effect of residence time by referring more to your own results in the first part. The first part sounds like general understanding / background.

[**Response**] Thanks for your comments and suggestions. Yes, we stated general understandings on the nitrogen limitation from plant N uptake and net N mineralization based on both steady- and nonsteady- state in the first half of this paragraph. For our analysis based on the steady state, we mainly discussed the three C-N schemes referring our results at the steady state in the latter of this paragraph. To make it clearer, we have revised this paragraph, and added "This N limitation mainly occurs in nonsteady state, because accumulation of N in the slow SOM pools reduces N available for plant uptake (Thomas et al., 2015). At or near the steady state, however, the sequestration of N in SOM mainly affects the C residence time (Fig. 8 and 10b). In this study, the different NUE among the three C-N schemes are induced by different mechanisms." In Lines 512-516.

- *L544- "This mechanism promotes respiration of the faster turnover pools": This sentence is not obvious for me. Why does the excess-C removal process in SM3 promote the respiration of the faster turnover pools?*

[**Response**] Sorry for the confusion. For the SM3 (O-CN model), the excess C is respired to prevent the accumulation of C beyond the storage capacity. At steady state, those SOM pools with faster turnover rates have smaller storage capacity than those with slower turnover rates. As a result, the excess C promotes the respiration of the faster turnover pools primarily. To make it clear in this study, we added "to prevent the accumulation of C beyond the storage capacity" in Line 567.

- *L557- "which is associated with plant competitiveness in SM1 and the respiration of excess labile C in SM3": how did you get to this conclusion? Readers will need more explanation on this.*

[**Response**] Thanks for your comments. Based on the traceability analysis (Eq.30 and Fig. 8), the baseline C residence time (and thus the C residence time Eq. 31) is calculated by allocation coefficients (*B* vector). Based on sensitivity analysis (Fig. 10b), the plant and microbe competition (PMC) and the plant tissue C:N (PS) have the highest sensitivities to C residence time for SM1 and SM3, respectively. For the SM3, the representation of respiration of excess labile C mainly drives the change of plant C:N ratio (Fig. 4f and 4l). In the revised version, we linked those results in Lines 580-581.

- *Just a suggestion: As you noted in L513, "The effects of ecosystem N status on C mean residence time, however, has been much less studied than N limitation on ~", the N impact on MRT has been unclear when understanding model's behavior. I suppose you can address more in your conclusion section that your analysis framework can quantify the degree of N regulation on C storage capacity, with breaking down it into BOTH primary production and*

MRT (as a steady state). I think this will give more significance to your work and could be a strong message for readers.

[**Response**] Thanks so much for your suggestions. In this revised version, we added more conclusion on the N regulation on ecosystem C storage capacity based on our results. We hope you will find our revision satisfactory.

Carbon-nitrogen coupling under three schemes of model representation: a traceability analysis

Zhenggang Du[1], Ensheng Weng[2], ~~Jianyang Xia[1*],~~ Lifen Jiang[3], Yiqi Luo[3,4], Jianyang Xia[1,5*], Xuhui Zhou[1,~~5~~6*]

[1]*Center for Global Change and Ecological Forecasting, Tiantong National Field Observation Station for Forest Ecosystem, School of Ecological and Environmental Sciences, East China Normal University, Shanghai 200062, China*

[2]*Department of Ecology & Evolutionary Biology, Princeton University, Princeton, NJ, USA*

[3]*Center for Ecosystem Science and Society, Northern Arizona University, AZ, USA*

[4]*Department for Earth System Science, Tsinghua University, Beijing 100084, China*

[5]*Forest Ecosystem Research and Observation Station in Putuo Island, School of Ecological and Environmental Sciences, East China Normal University, Shanghai 200062, China*

~~[5]Shanghai~~ [6]*Shanghai Institute of Pollution Control and Ecological Security, 1515 North Zhongshan Rd, Shanghai 200437, China*

***For correspondence:**

Xuhui Zhou & Jianyang Xia

School of Ecological and Environmental Sciences

East China Normal University

500 Dongchuan Road, Shanghai 200062, China

Email: xhzhou@des.ecnu.edu.cn, jyxia@des.ecnu.edu.cn

Tel/Fax: +86 21 54341275

Abstract The interaction between terrestrial carbon (C) and nitrogen (N) cycles has been incorporated into more and more land surface models. However, the scheme of C-N coupling differs greatly among models, and how these diverse representations of C-N interactions will affect C-cycle modeling remains unclear. In this study, we explored how the simulated ecosystem C storage capacity in the terrestrial ecosystem (TECO) model varied with three different commonly-used schemes of C-N coupling. The three schemes (SM1, SM2, and SM3) have been used in three different coupled C-N models (i.e., TECO-CN, CLM 4.5, and O-CN, respectively). They differ mainly in the stoichiometry of C and N in vegetation and soils, plant N uptake strategies, down-regulation of photosynthesis, and the pathways of N import. We incorporated the three C-N coupling schemes into the C-only version of TECO model, and evaluated their impacts on the C cycle with a traceability framework. Our results showed that all of the three C-N schemes caused significant reductions in steady-state C storage capacity compared with the C-only version with the magnitudes of -23%, -30% and -54% for SM1, SM2, SM3, respectively. These reduced C storage capacity was mainly derived from the combined effects of decreases in net primary productivity (NPP, -29%, -15% and -45%) and changes in mean C residence time (MRT, 9%, -17% and -17%) for SM1, SM2, and SM3, respectively. The differences in NPP are mainly attributed to the different assumptions on plant N uptake, plant tissue C:N ratio, down-regulation of photosynthesis, and biological N fixation. In comparison, the alternative representations of the plant vs. microbe competition strategy and the plant N uptake, combining with the flexible C:N ratio in vegetation and soils, led to a notable spread MRT. These results highlight that the diverse assumptions on N processes represented ~~among~~ by different C-N coupled models could cause additional uncertainty to land surface models. Understanding their difference can help us improve the capability of models to predict future biogeochemical cycles of terrestrial ecosystems.

Keywords: carbon-nitrogen coupling, traceability analysis, carbon storage capacity, nitrogen limitation, carbon residence time

1. Introduction

~~The t~~Terrestrial ecosystem carbon (C) storage is jointly determined by ecosystem C input (i.e., net primary productivity, NPP) and mean residence time (MRT), both of which are strongly affected by the terrestrial nitrogen (N) availability (Vitousek et al., 1991; Hungate et al., 2003; Luo et al., 2017). Nitrogen is an essential component of enzymes, proteins, and secondary metabolites (van Oijen and Levy, 2004). Plant and microbial production require N to meet their stoichiometric demands, thus affecting the C balance and nutrient turnover of ecosystems (Cleveland et al., 2013; Wieder et al., 2015b). Since N limitation is widespread for plant growth in terrestrial ecosystems (LeBauer et al., 2008; Xia and Wan, 2008), N availability is often highly correlated with key ecological processes, such as C assimilation (Field and Mooney, 1986; Du et al., 2017), allocation (Kuzyakov et al., 2013), plant respiration (Sprugel et al., 1996), and litter and soil organic matter (SOM) decomposition (Terrer et al., 2016). Nitrogen dynamics thus plays an important role in governing the terrestrial ecosystem C storage (García-Palacios et al., 2013; Shi et al., 2015).

Given the importance of N availability on C sink projections (Hungate et al., 2003; Wang and Houlton 2009, Zaehle et al., 2015, Wieder et al., 2015b), N processes are increasingly incorporated into biogeochemical models. The representation of N cycling and their feedback to C cycling in models reflects what has been established in the ecosystem research community. Early C-N coupled models demonstrated that the N availability limited C storage capacity with associated effects on plant photosynthesis and growth in many terrestrial ecosystems (Melillo et al., 1993; Luo et al., 2004). Recent studies have largely confirmed these results by improving C-N coupling models with multiple hypotheses (Zhou et al., 2013; Zaehle et al., 2014; Thomas et al., 2015). These hypotheses include the plant down-regulation productivity based on N required for cell construction or N availability for plant absorption (Thornton et al., 2009; Gerber et al., 2010), constant or flexible stoichiometry for allocation and tissue (Wang et al., 2001; Shevliakova et al., 2009; Zaehle et al., 2010), competition between plants and microbes for soil nutrients (Zhu et al., 2017), Evapotranspiration (ET)- or NPP-driven empirical functions to generate spatial estimates of biological N fixation (BNF) (Cleveland et al., 1999; Wieder et al., 2015a; Meyerholt et al., 2016), and respiration of excess C to obtain N from environment and/or to prevent the accumulation of C beyond the storage capacity (Zaehle et al., 2010). The knowledge has significantly helped improve our understanding of the terrestrial C-N coupling and is an important basis to develop comprehensive terrestrial process-based models (Thornton et al., 2007; Thomas et al., 2013).

However, simulated results of the terrestrial C cycle illustrated considerable spread among models, and much of uncertainty arose from predictions of N effects on C dynamics (Arora et al., 2013; Zaehle et al., 2015). The contradictory results were largely from different representations of fundamental N processes (e.g., the degree of flexibility of C:N ratio in vegetation and soils, plant N uptake strategies, pathways of N import, decomposition, and the representations of the competition between plants and microbes for mineral N) (Sokolov et al., 2008; Wania et al., 2012; Walker et al., 2015). Furthermore, the methodology used to derive the C-N coupling schemes among models varied largely, which might be invalid for the model intercomparisons to provide insight into the underlying mechanism of N status for terrestrial C cycle projection.

In the past decades, terrestrial models integrated more and more processes to improve model performance (Koven et al., 2013; Todd-Brown et al., 2013; Wieder et al., 2014). The more processes incorporated, the more difficult it becomes to understand or evaluate model behavior (Luo et al., 2015). The traceability analysis has been developed to diagnose the simulation results within (Xia et al. 2013; Ahlström et al., 2015) and among (Rafique et al., 2016; Zhou et al., 2018) models. Based on the traceability analysis framework, key traceable elements, including fundamental properties of the terrestrial C cycle and their representations in shared structures among existing models, can be identified and characterized under different sources of variation (e.g., external forcing and uncertainty in processes) ~~compared to the achieved predictive ability~~. The traceability analysis enables diagnosis of where models are clearly lacking predictive ability and evaluation of the relative benefit when more or alternative components are added to the models (Luo et al., 2015).

This study is designed to examine the effects of C-N coupling under different schemes of model representation on ecosystem C storage in the Terrestrial Ecosystem (TECO) model with the traceability analysis framework. Three schemes of model representation were conducted mainly based on carbon-nitrogen coupling version of TECO (TECO-CN ~~(SM1)~~, Weng and Luo, 2008, [SM1]), Community Land Model Version 4.5 (CLM 4.5 ~~(SM2)~~, Koven et al., 2013; Oleson et al., 2013, [SM2]) and carbon-nitrogen coupling version of the Organizing Carbon and Hydrology in Dynamic Ecosystems model (O-CN ~~(SM3~~, Zaehle and Friend, 2010; Zaehle et al., 2011, [SM3]) (Table 1). The three C-N schemes differ in degrees of flexibility of C:N ratio in vegetation and soils, plant N uptake strategies, pathways of N import, and the representations of the competition between plants and microbes for soil available N. Based on the forcing data of ambient CO_2 concentration, N deposition, and

meteorological data (i.e., air temperature, soil temperature, relative humidity, vapour pressure deficit, precipitation, wind speed, photosynthetically active radiation) obtained from Duke Forest during the period of 1996-2007, we conduct three alternative C-N coupling schemes (i.e., SM1, SM2 and SM3) as well as C-only in TECO model framework to compare their effects on the ecosystem C storage capacity. The N-processes sensitivity analysis was carried out to evaluate the variability in estimated ecosystem C storage caused by the process-related parameters at the steady state.

2. Materials and methods

2.1 Data sources

The datasets used in this study were taken from the Duke free-air CO_2 enrichment (FACE) experiment, located in the Blackwood Division, North Carolina, USA (35.97^o N, 79.08^o W). The flux tower lies on a 15-year-old loblolly pine (*Pinus taeda L.*) plantation. The meteorological forcing data were downloaded from the AmeriFlux database at http://ameriflux.lbl.gov, including ambient CO_2 concentration ([CO_2]), air temperature at the top canopy (*Ta*), soil temperature (*Ts*), photosynthetically active radiation (*PAR*), relative humidity (*RH*), vapor pressure deficit (*VPD*), precipitation, wind speed [*Ws*], and N deposition. All forcing data sets are available from 1996 to 2007. To set the initial condition for the models, we collected the related datasets from the previous studies. Standing biomass and biomass production data at each plot for plant compartments (i.e., foliage, fine root and woody biomass, including branches and coarse roots) were taken from McCarthy et al. (2010). The C and N concentration data for each plant compartment based on Finzi et al. (2007) were used to estimate C and N stocks and fluxes. Plant N demand and uptake were calculated from these data measured by Finzi et al. (2007). The C and N concentrations of litter and SOM were obtained from Lichter et al. (2008).

2.2 Model description and C-N schemes

2.2.1 TECO-CN

The terrestrial ecosystem C-N coupling model (TECO-CN) used in the present study is a variant of the TECO-Carbon-only version (TECO-C) by incorporating additional key N processes (Fig. 1). TECO-C model is a process-based ecosystem model designed to examine critical processes regulating interactive responses of plants and ecosystems to climate change. It has four major components: canopy photosynthesis module, plant growth module, soil water dynamic module, and soil C dynamic module. The canopy photosynthesis and soil

water dynamic modules run at hourly time step while the plant growth and soil C dynamic modules run at the daily time step. The detailed description of the TECO-C model can be found in Weng and Luo (2008).

The N cycle added to the TECO model for this study is simplified following the structure of Luo ~~&~~ and Reynolds (1999), Gerber et al. (2010), and Wang et al. (2010). It has a similar structure to the TECO-C model (Fig. 1). There are nine organic N pools ~~and one inorganic soil N pool~~, including plant, litter and soil N pools, and one inorganic soil N pool. The plant N pools include leaves, wood, roots, and mineral N in plant tissues. The litter and soil N pools include metabolic and structural litter N, fast, slow, and passive soil organic N (SON), and soil mineral N pools. The total plant N demand on each time step is calculated following the NPP allocation to new tissue growth based on their C:N ratios. To meet the demand, the plant N supply is calculated from three parts, including the retranslocated N from senescing tissues, plant uptake from soil mineral N pool, and external N sources from atmospheric deposition and biological N fixation. The N absorbed by roots enters into the mineral N pool in plant tissues, and then is allocated to the remaining plant pools with plant growth. The N in leaves and fine roots is reabsorbed before senescence. Plant litters will enter metabolic or structural pools depending on their C:N ratios.

The allocation coefficients act as the key factor to determine the baseline C residence time in this study. Plant assimilated C allocating to the leaves, stems and roots depends on their growth rates, which vary with phenology (Luo et al., 1995; Denison and Loomis, 1989; Shevliakova et al., 2009; Weng and Luo, 2008):

$$b_l = \frac{1}{1+c_1+c_2} \quad (1)$$

$$b_s = \frac{c_2}{1+c_1+c_2} \quad (2)$$

$$b_r = \frac{c_1}{1+c_1+c_2} \quad (3)$$

where b_l, b_s and b_r are the partitioning coefficient of newly assimilated C to leaves, stems and roots, respectively. Parameters c_1 and c_2 are calculated as:

$$c_1 = \frac{bm_l}{bm_r} * \frac{CN_l^i}{CN_l^0} \quad (4)$$

$$c_2 = 0.5 * 250e^3 * SLA * 0.00021 * h^2 \quad (5)$$

where bm_l and bm_r are the leaf and root biomass; CN_l^i and CN_l^0 represent the C:N ratios of the leaf pool at 0 and current time step, respectively; SLA is specific leaf area; h is plant height, which is calculated as:

$$h = h_{max}(1 - \exp(-h_1 * bmP)) \quad (6)$$

where h_{max} is the maximum canopy height; h_1 is an empirical parameter and bmP is plant biomass.

2.2.2 C-N coupling schemes

We conducted four experiments including three simulations with their representations of C-N coupling schemes (SM1, SM2 and SM3) and an additional C-only simulation in TECO model framework. The three C-N interaction simulations include one original scheme in TECO-CN model and the other two schemes representing CLM4.5-BGC and O-CN. The three C-N coupling schemes differ in the representation of down-regulation of photosynthesis, the degree of flexibility of C:N ratio in vegetation and soils (i.e., fixed C:N ratio in SM2, flexible C:N ratio in SM1 and SM3), plant N uptake strategies, pathways of N import to the plant reserves, and the competition between plants, and microbes for soil mineral N (Table1, Fig. 2).

SM1 (TECO-CN)

The N down-regulation of photosynthesis in SM1 is determined by the comparison between plant N demand and actual supply of N:

$$f_{dreg} = \min(\frac{N_{sup}}{N_{demand}}, 1) \quad (7)$$

where N_{sup} (g N m^{-2} s^{-1}) is actual supply of N obtained from re-translocated N, plant N uptake, and biological N fixation. N_{demand} (g N m^{-2} s^{-1}) is plant N demand, which is calculated as:

$$N_{demand} = \sum_{i=leaf,wood,root} \frac{C_i}{CN_i^0} \quad (8)$$

where C_i is the C pool size of plant tissue at the current time step, and CN_i^0 is the C:N ratio of plant tissue at the ~~last~~ first time step.

The re-translocated N is calculated as:

$$N_{retrans} = \sum_{i=leaf,wood,root} r_i \times outC_i/CN_i \quad (9)$$

where r_i is the N resorption coefficient, CN_i is the C:N ratio and $outC_i$ (g C m^{-2} s^{-1}) is the value of C leaving plant pool *i* at each time step.

The plant N uptake (g N m^{-2} s^{-1}) from soil mineral N pool is a function of root biomass density ($Root_{total}$, g C m^{-2}) and N demand of plants, following McMurtrie *et al*. (2012)

$$N_{uptake} = min(\max(0, N_{demand} - N_{retrans}), f_{\mathrm{U,max}} \times SN_{\mathrm{mine}} \times \frac{Root_{\mathrm{total}}}{Root_{\mathrm{total}}+Root_0}) \quad (10)$$

where N_{demand} is the N demand of plants; SN_{mine} (g N m^{-2}) is the soil mineral N; $f_{\mathrm{U,max}}$ is the maximum rate of N absorption per step when $Root_{total}$ approaches infinity; and $Root_0$ (g C m^{-2}) is a constant of root biomass at which the N-uptake rate is half of the parameter $f_{\mathrm{U,max}}$.

The biological N fixation (g N m^{-2} s^{-1}) is calculated as:

$$N_{BNF} = \min(\max(0, N_{demand} - N_{retrans} - N_{uptake}), n_{fix} \times f_{nsc} \times NSC) \quad (11)$$

where $n_{fix} = 0.0167$ is the maximum N fixation ratio and f_{nsc} is the nutrient limiting factor. f_{nsc} is calculated as

$$f_{nsc} = \begin{cases} 0, & NSC < NSC_{min} \\ \frac{NSC-NSC_{min}}{NSC_{max}-NSC_{min}}, & NSC_{min} < NSC < NSC_{max} \\ 1, & NSC > NSC_{max} \end{cases} \quad (12)$$

where NSC_{min} (g C m^{-2}) and NSC_{max} (g C m^{-2}) are the minimal and maximal sizes of nonstructural C pool, respectively.

The soil microbial immobilization (g N m^{-2} s^{-1}) is calculated as:

$$Imm_N = \begin{cases} \sum_{i=4}^{8} min\left(\left(\frac{C_i}{CN0_i} - \frac{C_i}{CN_i}\right), 0.1 * SN_{min}\right) for\ CN_i \geq CN0_i \\ \sum_{i=4}^{8} min\left(\left(\frac{C_i}{CN_i} - \frac{C_i}{CN0_i}\right), 0.1 * SN_{min}\right) for\ CN_i < CN0_i \end{cases} \quad (13)$$

where $CN0_i$ and CN_i $(i = 4, 5, 6, 7, 8)$ are the C:N ratios of metabolic litter, structural litter, fast, slow and passive soil organic C pools at first- and current-time step, respectively.

Two pathways of N loss are modeled. One is gaseous loss (N_{gas_loss}, g N m^{-2} s^{-1}) and another is leaching (N_{leach}, g N m^{-2} s^{-1}). Both are proportional to the availability of soil mineral N (SN_{min}, g N m^{-2}). The equations are:

~~$N_{gas\_loss} = f_{ngas} \times e^{\frac{T_{soil}-25}{10}} \times SN_{min}$ (14)~~

$$N_{leach} = f_{nleach} \times \frac{V_{runoff}}{h_{depth}} \times SN_{min} \quad (15\,14)$$

$$N_{gas\_loss} = \max(f_{ngas} \times e^{\frac{T_{soil}-25}{10}} \times SN_{min}, N_{BNF}+N_{depos}-N_{leaching}) \quad (15\,14)$$

where $f_{ngas} = 0.001$ and $f_{nleach} = 0.5$, T_{soil}(°C) is the soil temperature, V_{runoff} (mm s^{-1}) is the value of runoff, and h_{depth} (mm) is the soil depth, Ndepos = 0.78 gN m^{-2} yr^{-1}, is N deposition used in this study. ~~.~~

SM2 (CLM4.5bgc)

The N down-regulation of photosynthesis in SM2 is calculated as:

$$f_{dreg} = \frac{CF_{allo} - CF_{avail\_alloc}}{CF_{GPP_{pot}}} \quad (16)$$

where CF_{allo} (g C m^{-2} s^{-1}) is the total flux of allocated C, which is determined by available mineral N. CF_{avail_alloc} (g C m^{-2} s^{-1}) is the potential C flux from photosynthesis, which can be allocated to new growth. $CF_{GPP_{pot}}$ (g C m^{-2} s^{-1}) is the potential gross primary productivity (GPP) when there is no N limitation.

The re-translocated N (g N m^{-2} s^{-1}) is calculated as:

$$N_{retrans} = \min(N_{demand} \times \frac{N_{retrans_{ann}}}{N_{demand_{ann}}}, N_{retrans\_avail}) \quad (17)$$

where $N_{retrans_{ann}}$(gN m^{-2} y^{-1}) is the previous year's annual sum of re-translocated N obtained from senescing tissues, $N_{demand_{ann}}$ (g N m^{-2} y^{-1}) is the previous year's annual sum of plant N demand. $N_{retrans\_avail}$ (g N m^{-2} s^{-1}) is the available re-translocated N in senescing tissues, which is calculated by the proportional of senescing tissues.

The plant N uptake (g N m^{-2} s^{-1}) is described as:

$$N_{uptake} = (N_{demand} - N_{retrans}) \times f_{plant\_demand} \quad (18)$$

where f_{plant_demand} is the fraction (from 0 to 1) of the plant N demand, which can be met given the current soil mineral N supply and competition with heterotrophs. f_{plant_demand} is set to be equal to the fraction of potential immobilization demand (f_{immob_demand}) that is calculated as:

$$f_{plant\_demand} = f_{immob\_demand} = \frac{SN_{min}}{N_{plant\_demand} + N_{immob\_demand}} \quad (19)$$

where N_{immob_demand} (g N m^{-2} s^{-1}) is the total potential N immobilization demand (i.e., total potential microbial N demand).

The biological N fixation (g N m^{-2} s^{-1}) is calculated as:

$$N_{BNF} = 1.8(1 - e^{-0.03 \times NPP_{py}}) \Big/ (86400 \times 365) \quad (20)$$

where NPP_{py} (g C m^{-2} y^{-1}) is the previous-year NPP.

SM3 (O-CN)

The N down-regulation of photosynthesis in SM3 is calculated as:

$$f_{dreg} = a + b \times N_{leaf/LAI} \quad (21)$$

where a and b are empirical constants, and $N_{leaf/LAI}$ (g N m^{-2}) is foliage N per unit leaf area.

The re-translocated N (g N m^{-2} s^{-1}) is calculated as:

$$N_{retrans} = \sum_{i=leaf,root} \tau_i \times f_{trans,i} \quad (22)$$

where τ (g N m^{-2} s^{-1}) is the foliage or roots shed each step. $f_{trans,leaf} = 0.5$ and $f_{trans,root} = 0.2$ are the fractions of N re-translocated when the tissue dies off.

The plant N uptake (g N m^{-2} s^{-1}) is calculated as:

$$N_{uptake} = v_{max} \times SN_{min} \times \left(k_{Nmin} + \frac{1}{SN_{min} \times K_{Nmin}}\right) \times f(T_{soil}) \times f(NC_{plant}) \times C_{root} \quad (23)$$

where $v_{max} = 0.514$ is maximum N uptake capacity per unit fine root mass (Zaehle and Friend 2010; Kronzucker et al., 1995, 1996), k_{Nmin} is the rate of N uptake not associated with Michaelis-Menten Kinetics, K_{Nmin} is the half saturation concentration of fine root N uptake. $f(T_{soil})$ is calculated as:

$$f(T_{soil}) = \exp\left(308.56 * \left(\frac{1}{56.02} - \frac{1}{T_{soil}+46.02}\right)\right) \quad (24)$$

where T_{soil} (°C) is soil temperature.

C_{root} (g C m^{-2}) is fine root mass. $f(NC_{plant})$ is the dependency of N uptake on plant N status, and is calculated as:

$$f(NC_{plant}) = \max\left(\frac{NC_{plant} - nc_{leaf,max}}{nc_{leaf,min} - nc_{leaf,max}}, 0\right) \quad (25)$$

where $nc_{leaf,min}$ and $nc_{leaf,max}$ are the minimum and maximum foliage N concentration, respectively. NC_{plant} (g N g^{-1}C) is taken as the mean N concentration of foliage, fine root, and labile N pools, representing the active and easily translocatable portion of plant N:

$$NC_{plant} = \frac{N_{leaf} + N_{root} + N_{labile}}{C_{leaf} + C_{root} + C_{labile}} \quad (26)$$

The biological N fixation (g N m^{-2} s^{-1}) is calculated as:

$$N_{BNF} = 0.1 \times \max(0.0234 \times 30 \times AET + 0.172, 0) / (86400 \times 365) \quad (27)$$

where AET (mm y^{-1}) is the mean annual evapotranspiration.

2.3 Traceability analysis framework

The traceability analysis framework was used to evaluate the variation of the modeled ecosystem C storage capacity under different C-N schemes (Fig. S1). According to the traceability analysis framework (Xia et al., 2013), the modeled C storage capacity can be traced to (i) a product of NPP and ecosystem residence time (τ_E). The latter τ_E can be further traced to (ii) baseline C residence time (τ_E'), which is usually preset in a model according to

vegetation characteristics and soil types, (iii) N scalar (ξ_N), (iv) environmental scalars (ξ) including temperature (ξ_T) and water (ξ_W) scalars, and (v) the external climate forcing. The framework for decomposing modeled C storage capacity into a few traceable components is built upon a pool- and flux- structure, which is adopted in all of the terrestrial C models. The structure can well be represented by a matrix equation (Luo et al., 2003; Luo and Weng, 2011):

$$\frac{dX(t)}{dt} = BU(t) - A\xi CX(t) \quad (28)$$

where $X(t) = (X_1(t), X_2(t), \dots, X_8(t))^T$ is an 8 × 1 vector describing eight C pool sizes in leaf, root, wood, metabolic litter, structural litter, fast, slow, and passive soil organic C, respectively, in the TECO model (Weng and Luo, 2008). $B = (b_1,\ b_2, b_3, 0, \dots, 0)^T$ represents the partitioning coefficients of the photosynthetically fixed C into different plant pools. *U(t)* is the input of fixed C via plant photosynthesis. *A* is an 8 × 8 matrix representing the C transfer between pools. ξ is an 8 × 8 diagonal matrix of control of plant N status and environmental scalars on C decay rate at each time step. *C* is an 8 × 8 diagonal matrix representing the C exit rates from a pool at each time step.

The C storage capacity equals to the sum of C in all pools at the steady state (X_{ss}), which can be obtained by making Eqn.(28) equal to zero as described in Xia et al. (2013):

$$X_{ss} = (A\xi C)^{-1} B U_{ss} \quad (29)$$

The vector U_{ss} is the ecosystem C influx at the steady state. The partitioning (*B* vector), transfer coefficients (*A* matrix), and exit rates (*C* matrix) in Eqn. (28) together determine the baseline C residence time (τ_E'):

$$\tau_E' = (AC)^{-1} B \quad (30)$$

The baseline C residence time (τ_E') in Eqn. (30), N scalars (ξ_N) and environmental scalars (ξ_E) values together determine the C residence time (τ_E):

$$\tau_E = \xi^{-1}\tau_E' = (\xi_N \times \xi_E)^{-1}\tau_E' \quad (31)$$

Thus, the C storage capacity is jointly determined by the ecosystem residence time (τ_E) and steady-state C influx (U_{ss}):

$$X_{ss} = \tau_E U_{ss} \quad (32)$$

The environmental scalar is further separated into the temperature (ξ_T) and water (ξ_W) scalars, which can be represented as:

$$\xi_E = \xi_T \times \xi_W \quad (33)$$

As the respiration and decomposition rate modifier, the N scalar is given by vector $\xi_N = (\xi_{N1}(t),\ \xi_{N2}(t), \ldots, \xi_{N8}(t))^T$. The component $\xi_{Ni}(t)$ quantifies the changes of N content at each time step compared with initial condition in the C pool *i*. It is calculated as:

$$\xi_{Ni} = \exp(-\frac{CN_i^0 - CN_i^n}{CN_i^0}) \quad (34)$$

where CN_i^0 and CN_i^n are the C:N ratio of the pool *i* at 0 and *n* time step, respectively.

2.4 Model simulations and sensitivity analysis

To obtain the modeled C storage capacity, we spun up the TECO model with the C-only and three C-N coupling schemes to the steady state using the semi-analytical solution method developed by Xia et al. (2012). In this study, the meteorological forcings of 1996-2007 with the time step of half an hour were used to run the models to the steady state. Once the simulations are spun up to the steady state, C and N fluxes and state variables as well as the matrix elements *A*, *C*, *B*, and ξ in Eqn.(29) from all time steps in the last recycle of the climate forcing were saved for the traceability analysis.

The sensitivities of both NPP and mean C residence time (MRT) as well as ecosystem C storage capacity to each main N process in three schemes were calculated as:

$$S_i^{NPP}(P) = \frac{NPP_i^+(P) - NPP_i^-(P)}{NPP_i^0} \quad (35)$$

$$S_i^{MRT}(P) = \frac{MRT_i^+(P) - MRT_i^-(P)}{MRT_i^0} \quad (36)$$

$$S_i^{ECSC}(P) = S_i^{NPP}(P) \times S_i^{MRT}(P) \quad (37)$$

where $S_i^{NPP}(P)$, $S_i^{MRT}(P)$, and $S_i^{ECSC}(P)$ $(i = 1, 2, 3)$ represent the sensitivities of NPP, MRT and ecosystem C storage capacity to the N-process *P* in the scheme *i*, respectively. NPP_i^0 and MRT_i^0 are the annual mean values of NPP and MRT at the steady state in the scheme *i*. $NPP_i^+(P)$ and $NPP_i^-(P)$ are the annual mean values of NPP that were simulated to steady state again in scheme *i* based on the value of the N-process *P* (i.e., list in Table 1) by increasing 50% and decreasing 50%, respectively. $MRT_i^+(P)$ and $MRT_i^-(P)$ are the annual mean values of MRTs that were simulated at the same way as NPP and calculated using Eqn.(30) and Eqn.(31). ~~NPP_i^0 and MRT_i^0 are the annual mean values of NPP and MRT at the steady state in the scheme *i*.~~

3. Results

3.1 Simulations of C and N dynamics at steady state

At the steady state, the dynamics of N fluxes and soil mineral N showed different patterns among three C-N schemes in the TECO model (Fig. 3). The simulated soil N mineralization and plant N uptake fluxes in SM2 displayed the largest daily variation (~~0.00~~1.5 and 0.~~000~~86 mg N $m^{-2}d^{-1}$, respectively) and annual mean values (1.26 and 0.23 g N $m^{-2}yr^{-1}$, respectively) among three C-N schemes. This variation mainly resulted from both the plant N demand and the available N in soil (Fig. 3g). ~~For~~ The dynamic of soil mineral N also drove the variation of the N leaching flux, which the SM1 showed the largest daily variation (~~0.0~~40 mg N $m^{-2}d^{-1}$) and annual mean value (0.36 g N $m^{-2}yr^{-1}$). However, the representation of biological N fixation (BNF) as an option when the plant uptake is not enough for growth led to ~~the biological N fixation (BNF) flux in SM1 showed~~ the largest daily variation (~~0.0~~28 mg N $m^{-2}d^{-1}$) but with the smallest annual value (0.04 g N $m^{-2}yr^{-1}$) in SM1 in comparison with other two~~among three~~ C-N schemes. Both the nitrogen balance requirement and the dynamic of soil mineral N resulted to the largest daily variation (1.97 mg N $m^{-2}d^{-1}$) and annual value of gaseous N loss (1.39 g N $m^{-2}yr^{-1}$) in SM3. The combined effect of flexible C:N ratio and soil mineral N drove the largest daily variation of N immobilization fluxes (1.3 mg N $m^{-2}d^{-1}$)~~N immobilization fluxes~~ in SM3 ~~displayed the largest daily variation (0.0013 g N $m^{-2}d^{-1}$)~~ and ~~SM1 showed~~ the largest annual mean value (1.15 g N $m^{-2}yr^{-1}$) in SM1. The dynamics of soil mineral N in SM2 and SM3 displayed the similar patterns on the daily and annual dynamics.

Compared with the TECO-C model, the three C-N coupling schemes introduced significant signs of N limitation on forest growth at the steady state but with varying magnitude (Fig. 4). Specifically, the three N schemes caused significant reductions in GPP (10%, 10% and 12% for SM1, SM2 and SM3, respectively) compared to the C-only TECO model. Similar response patterns were also found on NPP, ecosystem respiration, and heterotrophic respiration. Among the three schemes, SM3 had the strongest effect (45%, 12% and 45% reduction for NPP, ecosystem respiration, and heterotrophic respiration, respectively), while SM2 had the weakest effect (15%, 8% and 13%, respectively) and the effect of SM1 was relatively moderate (29%, 10% and 29%, respectively). However, by comparison with the TECO-C version, both the SM1 and ~~SM2~~ SM3 schemes increased the autotrophic respiration by 12% and 27%, respectively. At or near the steady state, NEE in both TECO-C and three C-N coupling schemes had similarly mean values (1.37, -0.13, 0.66 and 0.84 g C m^{-2} yr^{-1}) which were equal to zero approximately but with large variations (56, 39.4, 48.1 and 34.9)~~., and SM2 scheme increased the NEE by 32%. Due to the NSC pool of TECO model, NEE were positive in all the experiments at the steady state (Weng and Luo, 2008)~~.

Three C-N coupling schemes induced different effects on C and N stoichiometric status for different pools (Figs. 5 and S2). All three schemes had significant limitation signs on woody, structural litter, fast and slow SOM pools but with different magnitudes (Fig. 5a). SM2 had the highest C sizes for the roots (731.8 g C m^{-2}) and metabolic litter (1252.1 g C m^{-2}), while SM1 had the highest C size for passive SOM pool (4249.5 g C m^{-2}). SM2 had the constant C:N ratios for all the displaying pools (Fig. 5b), while the C:N ratios for three displaying pools (leaf, root and structural litter) had no significant change in both SM1 and SM3. As for both woody and metabolic litter pools, SM1 and SM3 had higher C:N ratios (357.2 and 357.9, respectively) compared with SM2 (354). SM1 had the lowest C:N ratio (4.6) for soil passive SOM pool among the three schemes.

The divergent effects of three C-N schemes on plant N uptake (Fig. 3), autotrophic respiration, and NPP (Fig. 4) lead to different N use efficiency (NUE) and carbon use efficiency (CUE) (Fig. 6). SM1 had the highest NUE (159.1 g C g^{-1} N), mainly resulting from its lowest plant N uptake. In contrast, SM3 had the lowest NUE (67.3 g C g^{-1} N) as a result of its smallest NPP. Because of the hypothesis of N uptake for free, SM2 had the highest CUE (0.54) among three C-N schemes, which was close to that in the C-only version (0.57). However, SM3 had the lowest CUE (0.35) due to both C cost for plant actively uptake N and the assumption that increase respiration to remove the excess C.

3.2 Simulation of C storage capacity

The ecosystem C storage capacity also differed greatly among the three C-N coupling schemes and the C-only version of TECO model (Fig. 7). The C-only version had the largest C storage capacity (19.5 Kg C m^{-2}) among the four simulations due to its highest NPP (879.9 g C m^{-2} yr^{-1}). The C storage capacity in SM1 (15.1 Kg C m^{-2}) was close to that in SM2 (13.7 Kg C m^{-2}). The SM3 had the lowest C storage capacity (8.9 Kg C m^{-2}) among the four simulations as a result of its smallest NPP (483.9 g C m^{-2} yr^{-1}) and relative short MRT (18.6 years). By comparison with the C-only version, the three C-N schemes all induced different reductions on NPP (-29%, -15% and -45% for SM1, SM2, SM3, respectively) and further reduced their ecosystem C storage capacity. For the MRT, SM1 exhibited positive effects (+9%) relative to that in the C-only version, while another two schemes induced negative ones (i.e., -16.9% in SM2 and -16.7% in SM3).

3.3. Ecosystem C residence time

690 Ecosystem C residence time (τ_E) is collectively determined by baseline residence time, N
691 scalar, and environmental scalars as shown in Eqn. (31). Specifically, differences in τ_E among
692 three C-N coupling schemes and C-only TECO model are determined by baseline residence
693 time and the effects of N scalar on eight plant C pools (Fig. 8). For example, SM1 had the
694 longest τ_E because the N scalar had very strong control on passive SOM. The baseline
695 residence time was further determined by the C allocation (Fig. 9). Overall, compared with
696 C-only version, the additional N processes enhanced the partitioning coefficient of NPP to
697 roots (33%, 82% and 53% for SM1, SM2 and SM3, respectively) but decreased the
698 partitioning coefficient to wood (-25%, -45% and -34%, respectively). Furthermore, the
699 decreased partitioning coefficient to wood ~~(b2)~~ regulated the variations of the baseline
700 residence time of wood, structural litter, slow and passive SOM. However, the increased
701 partitioning coefficient to roots ~~(b3)~~ determined the variations of the baseline residence time
702 of roots and metabolic litter.
703
704 **3.4. Sensitivity of N processes to NPP and MRT**
705 For either NPP or MRT, the N processes had different sensitivities among the three C-N
706 schemes of TECO model (Fig. 10). For NPP, plant C:N ratio had the highest sensitivities in
707 both SM1 (0.32) and SM2 (0.53). However, plant N uptake in SM3 had the highest
708 sensitivity (0.87) for NPP. For MRT, competition between plants and microbes, down-
709 regulation of photosynthesis and plant C:N had the highest sensitivities in SM1 (0.27), SM2
710 (0.19) and SM3 (0.56), respectively. As the NPP and MRT jointly determined the ecosystem
711 C storage capacity, the plant tissue C:N ratio, down-regulation of photosynthesis, and plant N
712 uptake had the highest sensitivities for the ecosystem C storage capacity in SM1 (0.06), SM2
713 (0.09) and SM3 (0.26), respectively.
714
715 **4. Discussions**
716 **4.1 Underlying N processes and plant production**
717 Gross or net primary production (i.e., GPP or NPP) is regulated by the amount of N
718 availability for plant growth through the N demand, which is set by the relative proportion of
719 biomass growth in the different plant components and their C:N stoichiometry (Zaehle et al.,
720 2014; Thomas et al., 2015). The limitation of equilibrium N on plant production reflects the
721 effects from multiple processes of the C-N interaction, mainly including down-regulation of
722 photosynthetic capacity by N availability, the ecosystem's balance of N inputs and losses
723 (i.e., net ecosystem N exchange), plant N uptake, soil N mineralization, and the C:N

stoichiometry of vegetation and soils. However, due to a lack of consensus on the nature of the mechanisms, the representation of these processes varies greatly among diverse models (Zaehle et al., 2014).

There are two common alternative assumptions for the down-regulation of photosynthesis that have been implemented in models: (1) the change in photosynthetic capacity is directly associated with the magnitude of plant available N (e.g., SM2), and (2) N limitation is associated with foliage N, which feeds back to limit photosynthetic capacity (e.g., SM1 and SM3). Our results showed that both assumptions had significant limitations with similar effects on GPP (Figs. ~~3a~~ 4a and ~~3g~~4g). The probable reason is that the TECO model calculates photosynthesis by light availability and carboxylation rate based on the Farquhar model (Farquhar et al., 1980). The effects of N stress under the TECO framework, either associated with plant available N or associated with foliage N concentration, are estimated according to limiting factors of photosynthetic biochemistry (the maximum rate of carboxylation, V_{cmax}, and the maximum rate of electron transport at saturating irradiance, ~~V~~J_{max}). The two assumptions of down-regulation of photosynthesis may have different time-dependent effects on GPP in nonsteady-state systems (Xu et al., 2012; Walker et al., 2017).

At or near the steady state, net ecosystem N exchange is driven by the processes of N input via deposition and fixation and N loss via leaching and volatilization (Zaehle et al., 2014; Thomas et al., 2015). Previous studies have stated that analyzing the steady-state condition is useful to understand N effects because the balance between external N sources and N losses determine whether an ecosystem is N limited (Rastetter et al., 1997; Menge et al., 2009; Thomas et al., 2015). In this study, divergent NPP responses among the three schemes might partly result from their different representations of BNF (Figs. 3 and 10). Specifically, SM2 and SM3 simulated BNF explicitly, which used modified empirical relationships of BNF with NPP and evapotranspiration (ET), respectively (Cleveland et al., 1999). These phenomenological relationships generally captured biogeographical observations of higher rates of BNF in humid environments with high solar radiation (Wieder et al., 2015a). However, the highest response of NPP in only ET-driven BNF (i.e., SM3) may illustrate that not only energetic but also C costs of 'fixing' atmospheric di-N (N_2) into a biologically usable form (NH_3) broadly affect NPP (Gutschick 1981, Rastetter et al., 2001). This was because SM3 considered C investments in BNF while SM2 did not. By contrast, for the nonsteady state, the NPP-driven BNF creates a positive feedback between BNF and NPP, possibly causing large impact on C dynamic and terrestrial C storage (Wieder et al., 2015a). On the other hand, SM1 applied a different strategy, which set BNF as an option when the

plant N uptake is not enough for growth in terms of C investment, leading to the highest plant NUE (Fig. 6a) but a lower response of BNF to NPP (Fig. 10a). Another driving factor of the net ecosystem N exchange is the N loss, which depends on the rate of leaching and volatilization. In this study, using the same formulation as proportion to the size of soil mineral N pool among the three schemes, the different annual mean magnitude of N leaching was more correlated to soil mineral N. In the original CLM4.5 and O-CN (Oleson et al., 2013; Zaehle et al., 2010), the soil mineral N pool is divided into two pools (ammonium and nitrate). The N leaching is only valid on the nitrate pool, while the ammonium pool is assumed to be unaffected by leaching. This hypothesis may reduce the correlation between leaching and total soil mineral N.

The processes of plant N uptake and net N mineralization determine how N moves through the plant-soil system, thereby triggering N limitation on plant growth and C storage capacity (Fig. 10). However, to our knowledge, exploring those processes exactly in models is limited by inadequate representation of above- and below-ground interactions that control the patterns of N allocation and whole-plant stoichiometry (Zaehle et al., 2014; Thomas et al., 2015). Plant tissue, litter, and SOM are the primary sinks of N in terrestrial ecosystems, while N in these forms is not directly available for plant uptake, leading to an increase in N demand for plant growth. These N must turn over to become available for plant uptake. Therefore, the time for N to stay in these unavailable pools controls the transactional delay between the incorporation of N into plant unavailable pool and becomes available for plant uptake. In this way, the residence time of N in SOM appears to be an important factor for governing plant growth. This N limitation mainly occurs in nonsteady state, because accumulation of N in slow turnover rate SOM pools reduces N available for plant uptake (Thomas et al., 2015). At or near steady state, however, the sequestration of N in SOM mainly affects the C residence time (Fig. 8 and 10b). In this study, the different NUE among three C-N schemes induced by different mechanisms. SM1 had the highest NUE due to the combined effects of plant N uptake based on C investment strategy (as described above) and flexible tissue C:N ratio. Nitrogen stress increased tissue C:N ratio (Fig. 5b), leading to a high microbial N immobilization and then a lower net N mineralization (Fig. 3), which allowed plant cell construction with a lower N requirement. However, this was not the case for the SM3 since both hypotheses of increasing respiration to remove the excess C under N stress and the higher C investment for the BNF lead to the decrease in C input and then limits the microbial immobilization for the passive SOM pool. The inclusion of flexible C:N stoichiometry appeared to be an important feature allowing models to capture responses of the ecosystem C

storage capacity to climate variability through adjusting the C:N ratio of nonphotosynthetic tissues or the whole-plant allocation among tissues (Figs. 9 and 10) with different C:N ratios (Zaehle and& Friend, 2010).

4.2 Ecosystem N status and C residence time

Ecosystem N status in models, including plant-available and unavailable N forms, is set by N inputs from N fixation and N deposition, N losses from leaching and denitrification, and N gain from the turnover of litter and SOM through tissue senescence and decomposition. As noted above, external N cycle (i.e., N inputs and N losses) couples the N processes within the plant-litter-SOM system, being mainly associated with the limitation of plant production (Vitousek et al., 2004; Vicca et al., 2012; Craine et al., 2015). The effects of ecosystem N status on C mean residence time (MRT), however, has been much less studied than N limitation on productivity of plants and soil organisms, because these effects involve various impacts on C transfer among pools and C release from each pool via decomposition and respiration (Thompson & Randerson, 1999; Xia et al., 2013). Therefore, the different impacts of ecosystem N status induce oscillating N limitation on MRT (Figs. 8 and 10) due to the inherently different assumptions of C-N interactions among three C-N coupling schemes (Zhou et al., 2012; Shi et al., 2018).

At the steady state, the different effects of N status on changes in modelled MRT can be attributed to: the different rate of soil N mineralization dependent on the total amount of N in SOM and its turnover time, immobilization based on the competition strategy between plants and microbes and their stoichiometry, and different deployment of reabsorbed N. The traceability framework in this study can trace those different effects into three components (i.e., climate forcing, N scalar ξ_N, and baseline MRT) based on three alternative C-N coupling schemes under the TECO model framework. Since the forcing data are identical, we assumed the same effects for this component in all four experiments.

In our study, the N scalar (ξ_N) was based on the dynamics of C:N ratios (Eqn. 34). Therefore, N scalar had no effect on MRT in SM2, resulting from the assumption of fixed C:N ratio in all C pools (Figs. 5b and 8c). In both SM1 and SM3, however, the N scalar had large effects on the SOM pool, which is probably related to different mechanisms. Specifically, N scalar in the SM1 had the contrasting effects on MRT of fast and passive SOM pools (i.e., negative vs. positive, respectively), which may largely be attributed to the plant and microbe competition strategy combining with a much larger passive SOM pool in TECO-CN model (Du et al., 2017; Zhu et al., 2017). Under N stress, the competition between

plants and microbes is expected to be intensified, resulting in increasing C:N ratio of nonphotosynthetic tissues (e.g., wood and root) and the vegetation~~total~~ C:N ratio. This effectively prevents N limitation of cell construction and corresponds to an increase in whole-plant NUE (Thomas et al., 2015). In this case, higher C:N ratio in those tissues lowers structural litter quality, leading to soil microbes to immobilize more N to maintain their stoichiometric balance (Hu et al., 2001; Manzoni et al., 2010). However, in the SM3, increased respiration acted as a mechanism to remove the excess C, which is a stoichiometry-based implementation to prevent the accumulation of labile C to prevent the accumulation of C beyond the storage capacity under N stress (Zaehle and~~&~~ Friend, 2010; Thomas et al., 2015). This mechanism promotes respiration of the faster turnover pools (fast and slow SOM pools, Fig. 5a), leading to increased C:N ratio and decreased MRT in these two pools (Fig. 8).

In the traceability framework, the baseline MRT is determined by the potential decomposition rates of C pools (*C* matrix), coefficients of C partitioning of NPP (*B* vector), and transfer coefficients between C pools (*A* matrix, Eqn. [30]. Xia et al., 2013). The matrices *A* and *C* are preset in the TECO model according to vegetation characteristics and soil texture (Weng and Luo., 2008). Therefore, the notable spread in baseline MRT across the C-N schemes was induced by the *B* vector, which was modified by different N-limitation assumptions (Eqns. 1-6). Conceptually, in order to meet the N demand, plants adjust NPP allocation to N absorption tissues (e.g., roots). In this study, three schemes all had similar trends of adjusting allocation C from wood to roots (Fig. 9), but with different mechanisms. For both SM1 and SM3, increased root C allocation was mainly driven by N uptake capacity, which is associated with plant competitiveness in SM1 (Fig. 10b) and the respiration of excess labile C in SM3 (Fig. 4f, 4l and 10b), respectively. However, for SM2, increasing root C allocation may occur in spin-up stage from plant adjustment to whole-plant allocation among tissues to fit fixed C:N ratio.

5. Conclusions

The C-N coupling has been represented in ecosystem and land surface models with different schemes, generating great uncertainties in model predictions. The most difference among terrestrial C-N coupling models occurs with the degree of flexibility of C:N ratio in vegetation and soils, plant N uptake strategies, down-regulation of photosynthesis, and the representations of the pathways of N import. In this study, we evaluated alternative representations of C-N interactions and their impacts on C cycle using the TECO model framework. Our traceability analysis showed that the different representations of C-N

coupling processes lead to divergent ~~effects~~ simulations of~~on~~ both plant production and C residence time, and thus the ecosystem C storage capacity. The plant production are mainly affected by the different assumptions on net ecosystem N exchange, plant N uptake, net N mineralization, and the C:N ratio of vegetation and soil. In comparison, the alternative representations of the plant and microbe competition strategy and plant N uptake, combining with the flexible C:N ratio in vegetation and soils, led to a notable spread effects on C residence time. Overall, the down-regulation of photosynthesis, plant tissue C:N ratio, plant N uptake and N re-~~tranlocation~~translocation ~~N~~ are the dominant processes of the ecosystem C storage capacity. Identifying the representations of main C-N processes under different schemes can help us improve the N-limitation assumptions employed in terrestrial ecosystem models and forecast future C sink in response to climate change.

Code availability. The code for TECO-CN and the three C-N coupling schemes is available at https://github.com/zgdu/TECO-CN-2.0-new.

Data availability. The data for this paper are available upon request to the corresponding authors.

Competing interests. The authors declare that they have no conflict of interest.

Acknowledgements

This work was financially supported by the National Key R&D Program of China (2017YFA0604600), the National Natural Science Foundation of China (31770559, 31722009, 41630528), National 1000 Young Talents Program of China, and the Fundamental Research Funds for Central Universities. Zhenggang Du also thanks the China Scholarship Council (201606140130) for scholarship support.

Figure legends

Figure 1. Schematic diagram of the terrestrial ecosystem carbon (C) and nitrogen (N) coupling model (TECO-CN). (A) Canopy module, (B) Plant growth module, (C) Soil water dynamics module, (D) Soil carbon-nitrogen coupling module. Rectangles represent the carbon and nitrogen pools. R_a, autotrophic respiration. R_h, heterotrophic respiration. Retr., re-translocation. NSC, nonstructural carbohydrate. MNP, mineral N in plant tissues. SOM, soil organic matter. * set N fixation as an option when the plant N uptake is not enough for growth in terms of C investment.

Figure 2. Schematic diagram illustrating the major carbon (C) and nitrogen (N) flows and stores in a terrestrial ecosystem, enclosing with alternative assumptions of N processes represent in SM1, SM2 and SM3, respectively. Light-blue arrows indicate C-cycle processes and red arrows show N-cycle processes.. Met./Str. Litter, metabolic and/or structural litters; SOM, soil organic matter. * set N fixation as an option when the plant N uptake is not enough for growth in terms of C investment in SM1, but go directly to soil mineral N pool in SM2 and SM3.

Figure 3. Simulated nitrogen fluxes and soil mineral nitrogen from three carbon-nitrogen coupling schemes (SM1, SM2 and SM3) in TECO-CN model for 1996 to 2007 at Duke Forest. Mineral., mineralization; BNF, biological N fixation; Imm., immobilization.

Figure 4. Simulated annual (a-f) and mean (g-l) carbon fluxes from carbon-only version and carbon-nitrogen coupled with three schemes (SM1, SM2 and SM3) of TECO model for 1996 to 2007 at Duke Forest. GPP, gross primary productivity; NPP, net primary productivity; NEE, net ecosystem exchange of CO_2; R-eco, ecosystem respiration; R-heter, heterotrophic respiration; R-auto, autotrophic respiration.

Figure 5. The annual average sizes of carbon pools (panel a) at the steady-state among 1996-2007 for C-only version and the three C-N schemes (SM1, SM2 and SM3) and the C:N ratio (panel b) of each carbon pools for the three C-N schemes (SM1, SM2 and SM3) in TECO-CN model.

Figure 6. The nitrogen use efficiency (NUE, panel a) in three C-N schemes of TECO model (SM1, SM2 and SM3) and the carbon use efficiency (CUE, panel b) at the steady-state among C-only version and the three C-N schemes of TECO model (SM1, SM2 and SM3).

Figure 7. Simulation of annual ecosystem carbon storage capacity for 1996 to 2006 at Duke Forest by carbon in flux (NPP, x axis) and ecosystem residence time (τ_E, y axis) in TECO model framework with three carbon-nitrogen coupling schemes (SM1, SM2 and SM3) and in TECO C-only model (C). Inset (a), ecosystem carbon residence time (τ_E) in SM1, SM2, SM3 and C-only model; inset (b), mean ecosystem carbon storage simulated among SM1, SM2, SM3 and C-only model; inset (c), relative change of NPP and ecosystem residence time simulated among three schemes compared with in C-only model.

Figure 8. Determination of carbon-pool residence times based on traceability framework in TECO C-N model with three C-N coupling schemes (SM1, SM2 and SM3) and TECO C-only model (C). Panel (a), baseline residence time; panel (b), mean residence time, and panel (c), nitrogen scalar.

Figure 9. Coefficients of partitioning of NPP to nonstructural C (NSC), root, woody and leaf in C-only model (C) and C-N coupling model with three schemes (SM1, SM2 and SM3).

Figure 10. The sensitivity of nitrogen processes to NPP (panel a), ecosystem residence time (τ_E, panel b), and ecosystem C storage capacity (panel c) among three carbon-nitrogen coupling schemes (SM1, SM2 and SM3). DRP, down-regulation of photosynthesis; PS, plant tissue C:N ratio; PNU, plant N uptake; PMC: plant and microbe competition; BNF, biological N fixation; RtrN, re-tranlocation N; SS, soil pool C:N ratio.

Reference

Ahlström, A., Xia, J., Arneth, A., Luo, Y. and Smith, B., 2015. Importance of vegetation dynamics for future terrestrial carbon cycling. Environmental Research Letters, 10(5), p.054019.

Arora, V.K., Boer, G.J., Friedlingstein, P., Eby, M., Jones, C.D., Christian, J.R., Bonan, G., Bopp, L., Brovkin, V., Cadule, P. and Hajima, T., 2013. Carbon–concentration and carbon–climate feedbacks in CMIP5 Earth system models. Journal of Climate, 26(15), pp.5289-5314.

Cleveland, C.C., Townsend, A.R., Schimel, D.S., Fisher, H., Howarth, R.W., Hedin, L.O., Perakis, S.S., Latty, E.F., Von Fischer, J.C., Elseroad, A. and Wasson, M.F., 1999. Global patterns of terrestrial biological nitrogen (N2) fixation in natural ecosystems. Global biogeochemical cycles, 13(2), pp.623-645.

Cleveland, C.C., Houlton, B.Z., Smith, W.K., Marklein, A.R., Reed, S.C., Parton, W., Del Grosso, S.J. and Running, S.W., 2013. Patterns of new versus recycled primary production in the terrestrial biosphere. Proceedings of the National Academy of Sciences, 110(31), pp.12733-12737.

Craine, J.M., Brookshire, E.N.J., Cramer, M.D., Hasselquist, N.J., Koba, K., Marin-Spiotta, E. and Wang, L., 2015. Ecological interpretations of nitrogen isotope ratios of terrestrial plants and soils. Plant and Soil, 396(1-2), pp.1-26.

Denison, R.F. and Loomis, R.S., 1989. An integrative physiological model of alfalfa growth and development. Publication/University of California, Division of Agriculture and Natural Resources (USA).

Du, Z., Zhou, X., Shao, J., Yu, G., Wang, H., Zhai, D., Xia, J., Luo, Y., 2017. Quantifying uncertainties from additional nitrogen data and processes in a terrestrial ecosystem model with Bayesian probabilistic inversion. Journal of Advances in Modeling Earth Systems, 9(1), 548-565.

Farquhar GD, Caemmerer SV, Berry JA., 1980. A biochemical model of photosynthetic CO_2 assimilation in leaves of C3 species. Planta, 149, 78–90.

Finzi, A.C., Norby, R.J., Calfapietra, C., Gallet-Budynek, A., Gielen, B., Holmes, W.E., Hoosbeek, M.R., Iversen, C.M., Jackson, R.B., Kubiske, M.E. and Ledford, J., 2007. Increases in nitrogen uptake rather than nitrogen-use efficiency support higher rates of temperate forest productivity under elevated CO2. Proceedings of the National Academy of Sciences, 104(35), pp.14014-14019.

García‐Palacios, P., Maestre, F.T., Kattge, J. and Wall, D.H., 2013. Climate and litter quality differently modulate the effects of soil fauna on litter decomposition across biomes. Ecology letters, 16(8), pp.1045-1053.

Gerber S, Hedin LO, Oppenheimer M, Pacala SW, Shevliakova E (2010) Nitrogen cycling and feedbacks in a global dynamic land model. Global Biogeochemical Cycles, 24, GB1001.GutschickVP., 1981. Evolved strategies of nitrogen fixation in plants Am. Naturalist 118 607–37.

Hararuk, O., Xia, J. and Luo, Y., 2014. Evaluation and improvement of a global land model against soil carbon data using a Bayesian Markov chain Monte Carlo method. Journal of Geophysical Research: Biogeosciences, 119(3), pp.403-417.

Hendrey, G.R., Ellsworth, D.S., Lewin, K.F. and Nagy, J., 1999. A free‐air enrichment system for exposing tall forest vegetation to elevated atmospheric CO2. Global Change Biology, 5(3), pp.293-309.

Huang, Y., Lu, X., Shi, Z., Lawrence, D., Koven, C.D., Xia, J., Du, Z., Kluzek, E. and Luo, Y., 2018. Matrix approach to land carbon cycle modeling: A case study with the Community Land Model. Global change biology, 24(3), pp.1394-1404.

Koven, C.D., Riley, W.J., Subin, Z.M., Tang, J.Y., Torn, M.S., Collins, W.D., Bonan, G.B., Lawrence, D.M. and Swenson, S.C., 2013. The effect of vertically resolved soil biogeochemistry and alternate soil C and N models on C dynamics of CLM4. Biogeosciences, 10(11), p.7109.

Kronzucker H. J., M. Y. Siddiqi, and A. D. M. Glass (1995), Kinetics Of NO3- Influx In Spruce, Plant Physiology, 109, 319-326

Kronzucker H. J., M. Y. Siddiqi, and A. D. M. Glass (1996), Kinetics of NH4+ influx in spruce, Plant Physiology, 110, 773-779.

Kuzyakov, Y. and Xu, X., 2013. Competition between roots and microorganisms for nitrogen: mechanisms and ecological relevance. New Phytologist, 198(3), pp.656-669.

LeBauer, D.S. and Treseder, K.K., 2008. Nitrogen limitation of net primary productivity in terrestrial ecosystems is globally distributed. Ecology, 89(2), pp.371-379.

Lichter J, Billings SA, Ziegler SE, Gaindh D, Ryals R, Finzi AC, Jackson RB, Stemmler EA, Schlesinger WH., 2008. Soil carbon sequestration in a pine forest after 9 years of atmospheric CO2 enrichment. Global Change Biology 14: 2910–2922.

Luo, Y., Meyerhoff, P.A. and Loomis, R.S., 1995. Seasonal patterns and vertical distributions of fine roots of alfalfa (Medicago sativa L.). Field Crops Research, 40(2), pp.119-127.

1000 Luo Y, Reynolds JF., 1999. Validity of extrapolating field CO2 experiments to predict carbon
1001 sequestration in natural ecosystems. Ecology, 80, 1568-1583.
1002 Luo, Y, LW. White, JG. Canadell, EH. DeLucia, DS. Ellsworth, A Finzi, J Lichter, and WH
1003 Schlesinger., 2003. Sustainability of terrestrial carbon sequestration: a case study in Duke
1004 Forest with inversion approach. Global biogeochemical cycles, 17(1).
1005 Luo, Y., Su, B.O., Currie, W.S., Dukes, J.S., Finzi, A., Hartwig, U., Hungate, B., McMurtrie,
1006 R.E., Oren, R.A.M., Parton, W.J. and Pataki, D.E., 2004. Progressive nitrogen limitation
1007 of ecosystem responses to rising atmospheric carbon dioxide. AIBS Bulletin, 54(8),
1008 pp.731-739.
1009 Luo, Y, and Weng E., 2011. Dynamic disequilibrium of the terrestrial carbon cycle under
1010 global change. Trends in Ecology & Evolution 26(2): 96-104.
1011 Luo, Y.Q., Randerson, J.T., Friedlingstein, P., Hibbard, K., Hoffman, F., Huntzinger, D.,
1012 Jones, C.D., Koven, C., Lawrence, D., Li, D.J. and Mahecha, M., 2012. A framework for
1013 benchmarking land models.
1014 Luo Y, Keenan T F., 2015. Smith M. Predictability of the terrestrial carbon cycle. Global
1015 change biology, 21(5): 1737-1751.
1016 McCarthy HR, Oren R, Johnsen KH, Gallet-Budynek A, Pritchard SG, Cook CW, LaDeau
1017 SL, Jackson RB, Finzi AC., 2010. Re-assessment of plant carbon dynamics at the Duke
1018 free-air CO2 enrichment site: interactions of atmospheric [CO2] with nitrogen and water
1019 vailability over stand development. New Phytologist 185: 514–528.
1020 McMurtrie RE, Iversen CM, Dewar RC, Medlyn BE, Nasholm T, Pepper DA, Norby RJ.,
1021 2012. Plant root distributions and nitrogen uptake predicted by a hypothesis of optimal
1022 root foraging. Ecology and Evolution, 2, 1235-1250.
1023 Melillo JM, McGuire AD, Kicklighter DW, Moore B III, Vorosmarty CJ, Schloss A., 1993.
1024 Global climate change and terrestrial net primary production. Nature, 363, 234–240.
1025 Menge DNL, Pacala SW, Hedin LO., 2009. Emergence and maintenance of nutrient
1026 limitation over multiple timescales in terrestrial ecosystems. The American Naturalist,
1027 173, 164–175.
1028 Meyerholt J, Zaehle S, Smith MJ., 2016. Variability of projected terrestrial biosphere
1029 responses to elevated levels of atmospheric CO2due to uncertainty in biological nitrogen
1030 fixation. Biogeosciences 13: 1491–1518.
1031 Oleson, K., Lawrence, M., Bonan, B., Drewniak, B., Huang, M., Koven, D., Levis, S., Li, F.,
1032 Riley, J., Subin, M. and Swenson, S., 2013. Technical description of version 4.5 of the
1033 Community Land Model (CLM).

van Oijen, M., and P. Levy., 2004. Nitrogen metabolism and plant adaptation to the environment: The scope for process-based modeling, in Nitrogen Acquisition and Assimilation in Higher Plants, Plant Ecophysiol. Ser., vol. 3, edited by S. Amaˆncio and I. Stulen, pp. 133– 147, Kluwer Acad., Dordrecht, Netherlands.

Parton WJ, Hanson PJ, Swanston C, Torn M, Trumbore SE, Riley W, Kelly R., 2010. ForCent model development and testing using the Enriched Background Isotope Study experiment. Journal of Geophysical Research 115: G04001.

Rastetter EB, Agren GI, Shaver GR., 1997. Responses of N-limited ecosystems to increased CO2: a balanced-nutrition, coupled-element-cycles model. Ecological Applications, 7: 444–460.

Rastetter EB, Vitousek PM, Field C, Shaver G, Herbert D, Agren GI., 2001. Resource optimization and symbiotic nitrogen fixation. Ecosystems, 4, 369–388.

Shevliakova, E., Pacala, S.W., Malyshev, S., Hurtt, G.C., Milly, P.C.D., Caspersen, J.P., Sentman, L.T., Fisk, J.P., Wirth, C. and Crevoisier, C., 2009. Carbon cycling under 300 years of land use change: Importance of the secondary vegetation sink. Global Biogeochemical Cycles, 23(2).

Shi, Z., Crowell, S., Luo, Y. and Moore, B., 2018. Model structures amplify uncertainty in predicted soil carbon responses to climate change. Nature communications, 9(1), p.2171.

Sokolov, A.P., Kicklighter, D.W., Melillo, J.M., Felzer, B.S., Schlosser, C.A. and Cronin, T.W., 2008. Consequences of considering carbon–nitrogen interactions on the feedbacks between climate and the terrestrial carbon cycle. Journal of Climate, 21(15), pp.3776-3796.

Sprugel, D. G., M. G. Ryan, J. R. Brooks, K. A. Vogt, and T. A. Martin., 1996. Respiration from the organ level to the stand, in Resource Physiology of Conifers, edited by K. Smith and T. M. Hinckley, pp. 255–299, Academic, San Diego, Calif.

Terrer, C., Vicca, S., Hungate, B.A., Phillips, R.P. and Prentice, I.C., 2016. Mycorrhizal association as a primary control of the CO2 fertilization effect. Science, 353(6294), pp.72-74.

Thomas, R.Q., Zaehle, S., Templer, P.H. and Goodale, C.L., 2013. Global patterns of nitrogen limitation: confronting two global biogeochemical models with observations. Global change biology, 19(10), pp.2986-2998.

Thomas, R.Q., Brookshire, E.J. and Gerber, S., 2015. Nitrogen limitation on land: how can it occur in Earth system models?. Global change biology, 21(5), pp.1777-1793.

Thompson, M.V. and Randerson, J.T., 1999. Impulse response functions of terrestrial carbon cycle models: method and application. Global Change Biology, 5(4), pp.371-394.

Thornton, P.E., Lamarque, J.F., Rosenbloom, N.A. and Mahowald, N.M., 2007. Influence of carbon‐nitrogen cycle coupling on land model response to CO2 fertilization and climate variability. Global biogeochemical cycles, 21(4).

Todd-Brown, K.E., Randerson, J.T., Post, W.M., Hoffman, F.M., Tarnocai, C., Schuur, E.A. and Allison, S.D., 2013. Causes of variation in soil carbon simulations from CMIP5 Earth system models and comparison with observations.

Vicca, S., Luyssaert, S., Penuelas, J., Campioli, M., Chapin III, F.S., Ciais, P., Heinemeyer, A., Högberg, P., Kutsch, W.L., Law, B.E. and Malhi, Y., 2012. Fertile forests produce biomass more efficiently. Ecology letters, 15(6), pp.520-526.

Vitousek P M, Howarth R W., 1991. Nitrogen limitation on land and in the sea: how can it occur?. Biogeochemistry, 13(2): 87-115.

Vitousek, P.M., 2004. Nutrient cycling and limitation: Hawai'i as a model system. Princeton University Press.

Walker, A.P., Zaehle, S., Medlyn, B.E., De Kauwe, M.G., Asao, S., Hickler, T., Parton, W., Ricciuto, D.M., Wang, Y.P., Wårlind, D. and Norby, R.J., 2015. Predicting long‐term carbon sequestration in response to CO2 enrichment: How and why do current ecosystem models differ?. Global Biogeochemical Cycles, 29(4), pp.476-495.

Walker, A.P., Quaife, T., Bodegom, P.M., De Kauwe, M.G., Keenan, T.F., Joiner, J., Lomas, M.R., MacBean, N., Xu, C., Yang, X. and Woodward, F.I., 2017. The impact of alternative trait‐scaling hypotheses for the maximum photosynthetic carboxylation rate (Vcmax) on global gross primary production. New Phytologist, 215(4), pp.1370-1386.

Wang S, Grant RF, Verseghy DL, Black TA. 2001. Modelling plant carbon and nitrogen dynamics of a boreal aspen forest in CLASS – the Canadian Land Surface Scheme. Ecological Modelling 142: 135–154.

Wang YP, Law RM, Pak B., 2010. A global model of carbon, nitrogen and phosphorus cycles for the terrestrial biosphere. Biogeosciences, 7, 2261–2282.

Wania, R., Meissner, K.J., Eby, M., Arora, V.K., Ross, I. and Weaver, A.J., 2012. Carbon-nitrogen feedbacks in the UVic ESCM. Geoscientific Model Development, 5(5), p.1137.

Weng E, Luo Y., 2008. Soil hydrological properties regulate grassland ecosystem responses to multifactor global change: A modeling analysis. Journal of Geophysical Research: Biogeosciences, 113(G3).

Wieder, W.R., Boehnert, J. and Bonan, G.B., 2014. Evaluating soil biogeochemistry parameterizations in Earth system models with observations. Global Biogeochemical Cycles, 28(3), pp.211-222.

Wieder, W.R., Cleveland, C.C., Lawrence, D.M. and Bonan, G.B., 2015a. Effects of model structural uncertainty on carbon cycle projections: biological nitrogen fixation as a case study. Environmental Research Letters, 10(4), p.044016.

Wieder, W.R., Cleveland, C.C., Smith, W.K. and Todd-Brown, K., 2015b. Future productivity and carbon storage limited by terrestrial nutrient availability. Nature Geoscience, 8(6), p.441.

Xia, J. Y., Wan, S. Q., 2008. Global response patterns of terrestrial plant species to nitrogen addition. New Phytologist, 179, 428-439.

Xia, J.Y., Luo, Y.Q., Wang, Y.P., Weng, E.S. and Hararuk, O., 2012. A semi-analytical solution to accelerate spin-up of a coupled carbon and nitrogen land model to steady state. Geoscientific Model Development, 5(5), pp.1259-1271.

Xia, J., Luo, Y., Wang, Y.P. and Hararuk, O., 2013. Traceable components of terrestrial carbon storage capacity in biogeochemical models. Global Change Biology, 19(7), pp.2104-2116.

Xu, C., Fisher, R., Wullschleger, S.D., Wilson, C.J., Cai, M. and McDowell, N.G., 2012. Toward a mechanistic modeling of nitrogen limitation on vegetation dynamics. PloS one, 7(5), p.e37914.

Zaehle, S. and Friend, A.D., 2010. Carbon and nitrogen cycle dynamics in the O‐CN land surface model: 1. Model description, site‐scale evaluation, and sensitivity to parameter estimates. Global Biogeochemical Cycles, 24(1).

Zaehle, S. and Dalmonech, D., 2011. Carbon–nitrogen interactions on land at global scales: current understanding in modelling climate biosphere feedbacks. Current Opinion in Environmental Sustainability, 3(5), pp.311-320.

Zaehle, S., Medlyn, B.E., De Kauwe, M.G., Walker, A.P., Dietze, M.C., Hickler, T., Luo, Y., Wang, Y.P., El‐Masri, B., Thornton, P. and Jain, A., 2014. Evaluation of 11 terrestrial carbon–nitrogen cycle models against observations from two temperate Free‐Air CO2 Enrichment studies. New Phytologist, 202(3), pp.803-822.

Zaehle, S., Jones, C.D., Houlton, B., Lamarque, J.F. and Robertson, E., 2015. Nitrogen availability reduces CMIP5 projections of twenty-first-century land carbon uptake. Journal of Climate, 28(6), pp.2494-2511.

Zhou, L., Zhou, X., Zhang, B., Lu, M., Luo, Y., Liu, L. and Li, B., 2014. Different responses of soil respiration and its components to nitrogen addition among biomes: a meta‐analysis. Global change biology, 20(7), pp.2332-2343.

Zhu, Q., Riley, W. J., & Tang, J., 2017. A new theory of plant–microbe nutrient competition resolves inconsistencies between observations and model predictions. Ecological Applications, 27(3), 875-886.

Zhou, S., Liang, J., Lu, X., Li, Q., Jiang, L., Zhang, Y., Schwalm, C.R., Fisher, J.B., Tjiputra, J., Sitch, S. and Ahlström, A., 2018. Sources of uncertainty in modeled land carbon storage within and across three MIPs: Diagnosis with three new techniques. Journal of Climate, 31(7), pp.2833-2851.

Zhou, X., Zhou, T. and Luo, Y., 2012. Uncertainties in carbon residence time and NPP-driven carbon uptake in terrestrial ecosystems of the conterminous USA: a Bayesian approach. Tellus B: Chemical and Physical Meteorology, 64(1), p.17223.

Table1. Summary of the nitrogen-carbon coupling schemes used and the representation of key processes in the carbon-nitrogen cycle.

	SM1 (TECO-CN)[a]	SM2 (CLM4.5)[b,c]	SM3 (O-CN)[d,e]
Down-regulation of photosynthesis by N availability (DRP)	Based on the comparison between plant N demand and actual supply	Based on the available soil mineral N relative to the N demanded to allocate photosynthate to tissue	Based on foliage N concentration, which varies with N deficiency
Plant tissue stoichiometry (PS)	Flexible plant C:N ratio	Fixed plant C:N ratio	Flexible plant C:N ratio
Plant N uptake (PNU)	Based on fine root biomass, soil mineral N and N demand of plant. Plants itself choose the strategy between uptake from soil mineral N and fix N_2 by comparing C investment	Based on N required to allocate NPP to tissue. Plants uptake N for free	Combining active and passive uptake of mineral N based on fine root C, soil mineral N, plant transpiration flux, increases with increased plant N demand
N competition between plants and microbes (PMC)	Microbes have first access to soil mineral N	Based on demand by both microbial immobilization and plant N uptake	Microbes have first access to soil mineral N, the competitive strength of plants increases under nutrient stress
Biological N fixation (BNF)	Based on the nitrogen demand of plants and maximum N fixing ratio considering nutrient concentration	$f(NPP)$	$f(ET)$
Deployment of re-translocated N (RtrN)	Fixed fraction of litter	Based on available N in the tissue and the previous year's annual sum of plant N demand	Fixed fraction of dying leaf and root tissue
Soil organic matter stoichiometry (SS)	Flexible soil C:N ratio	Fixed soil C:N ratio	Flexible soil C:N ratio
N leaching	Function of soil mineral N pool and runoff	Function of soil mineral N pool and runoff	Function of soil mineral N and runoff
***Gaseous N loss**	Based on function of soil mineral N pool and soil temperature, and N deficit	Based on function of soil mineral N pool and soil temperature, and N deficit	Based on function of soil mineral N pool and soil temperature, and N deficit

[a]See this study; [b]Koven et al. (2013), [c]Oleson et al. (2013); [d] Zaehle and&Friend (2010), [e]Zaehle et al. (2011). *, use the same representation as in TECO-CN model among three schemes.

C, carbon; N, nitrogen; NPP, net primary productivity; ET, evapotranspiration.

Figure 1. TECO-CN

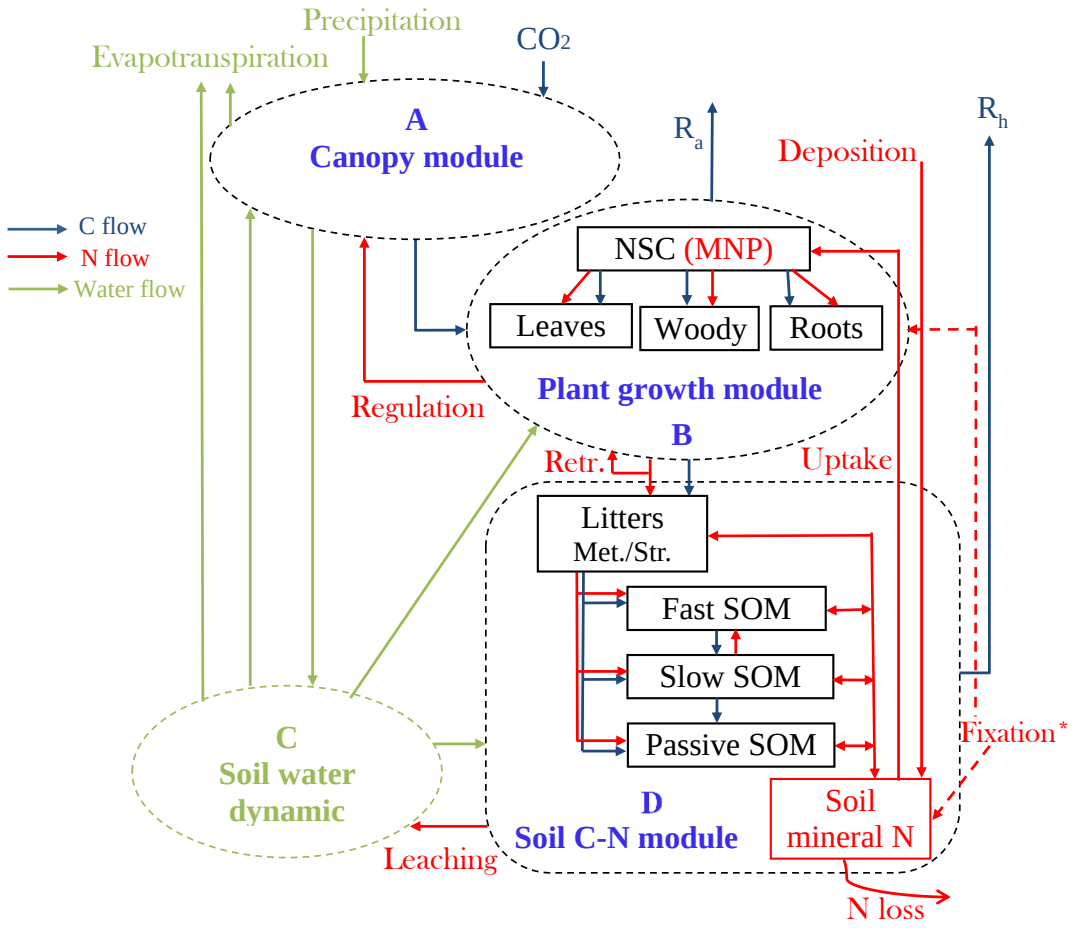

Figure 1. Schematic diagram of the terrestrial ecosystem carbon (C) and nitrogen (N) coupling model (TECO-CN). (A) Canopy module, (B) Plant growth module, (C) Soil water dynamics module, (D) Soil carbon-nitrogen coupling module. Rectangles represent the carbon and nitrogen pools. R_a, autotrophic respiration. R_h, heterotrophic respiration. Retr., re-translocation. NSC, nonstructural carbohydrate. MNP, mineral N in plant tissues. SOM, soil organic matter. * set N fixation as an option when the plant N uptake is not enough for growth in terms of C investment.

Figure 2

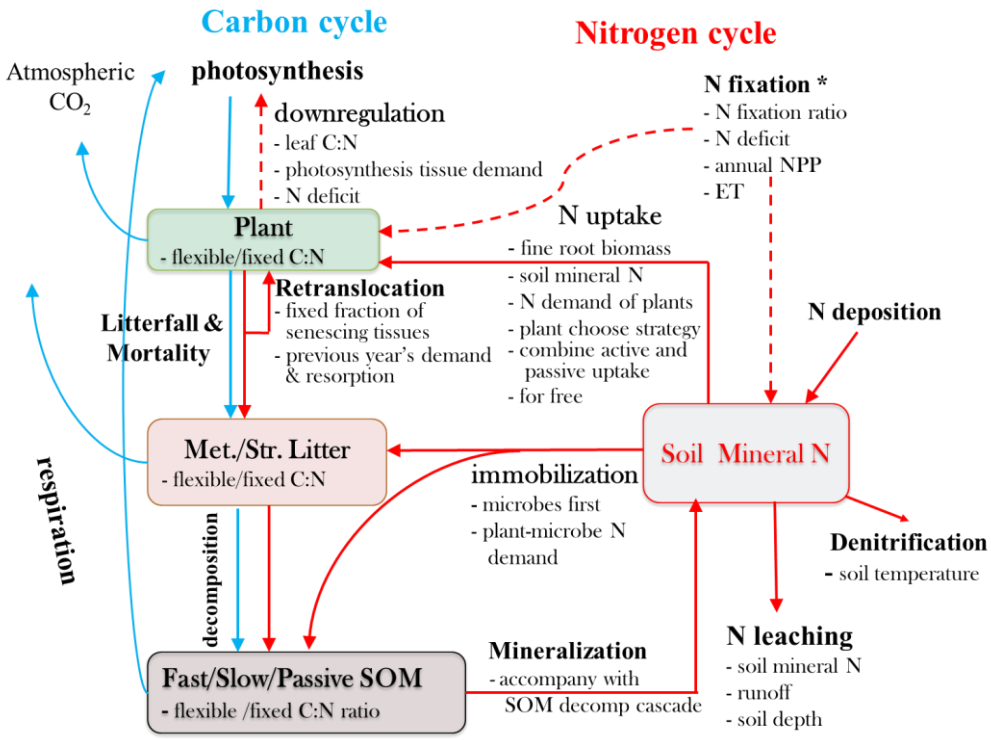

Figure 2. Schematic diagram illustrating the major carbon (C) and nitrogen (N) flows and stores in a terrestrial ecosystem, enclosing with alternative assumptions of N processes represent in SM1, SM2 and SM3, respectively. Light-blue arrows indicate C-cycle processes and red arrows show N-cycle processes. Met./Str. Litter, metabolic and/or structural litters; SOM, soil organic matter. * set N fixation as an option when the plant N uptake is not enough for growth in terms of C investment in SM1, but go directly to soil mineral N pool in SM2 and SM3.

Figure 3

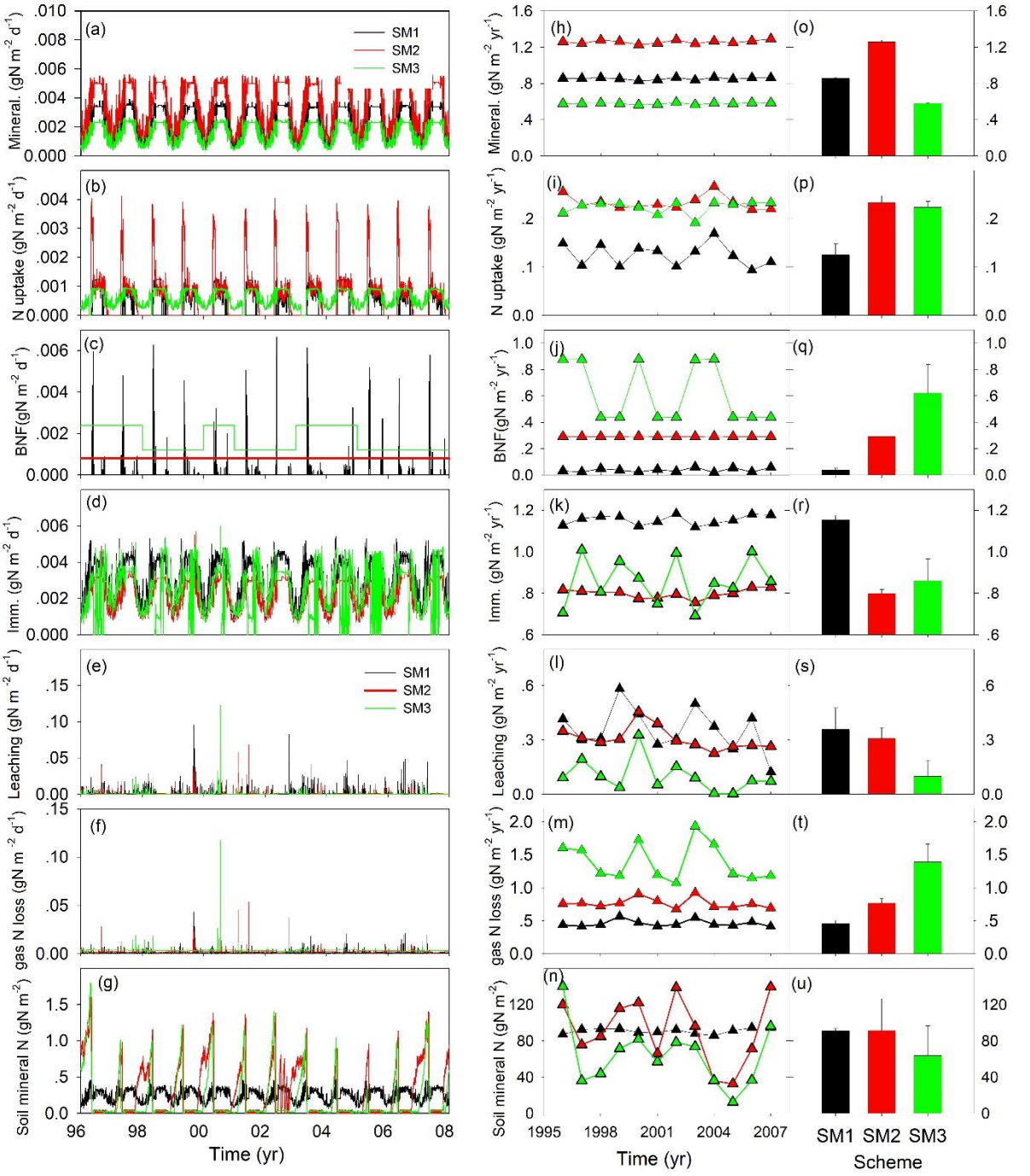

Figure 3. Simulated nitrogen fluxes and soil mineral nitrogen from three carbon-nitrogen coupling schemes (SM1, SM2 and SM3) in TECO-CN model for 1996 to 2007 at Duke Forest. Mineral., mineralization; BNF, biological N fixation; Imm., immobilization.

Figure 4

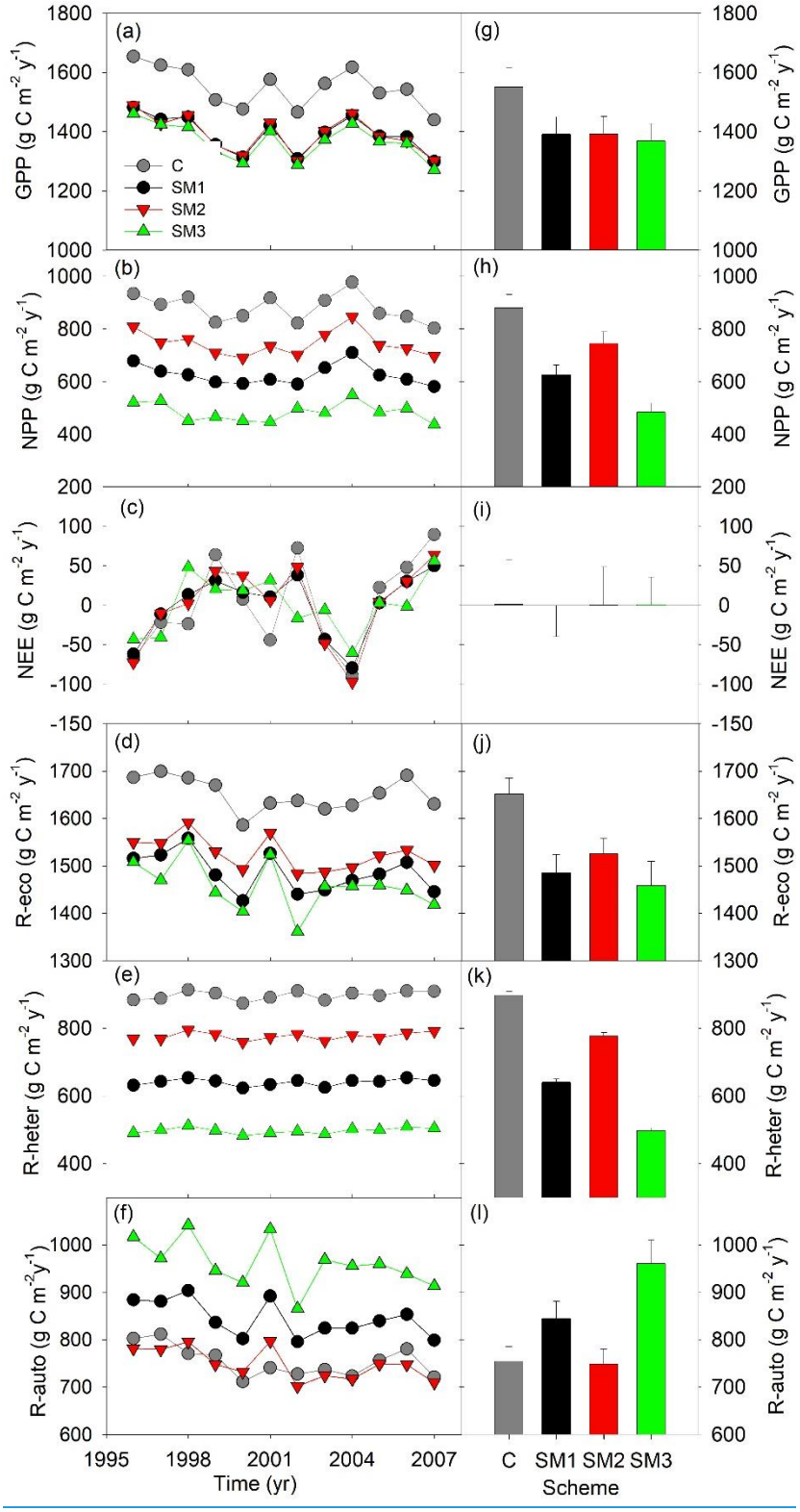

Figure 4. Simulated annual (a-f) and mean (g-l) carbon fluxes from carbon-only version and carbon-nitrogen coupled with three schemes (SM1, SM2 and SM3) of TECO model for 1996 to 2007 at Duke Forest. GPP, gross primary productivity; NPP, net primary productivity;

NEE, net ecosystem exchange of CO_2; R-eco, ecosystem respiration; R-heter, heterotrophic respiration; R-auto, autotrophic respiration.

Figure 5

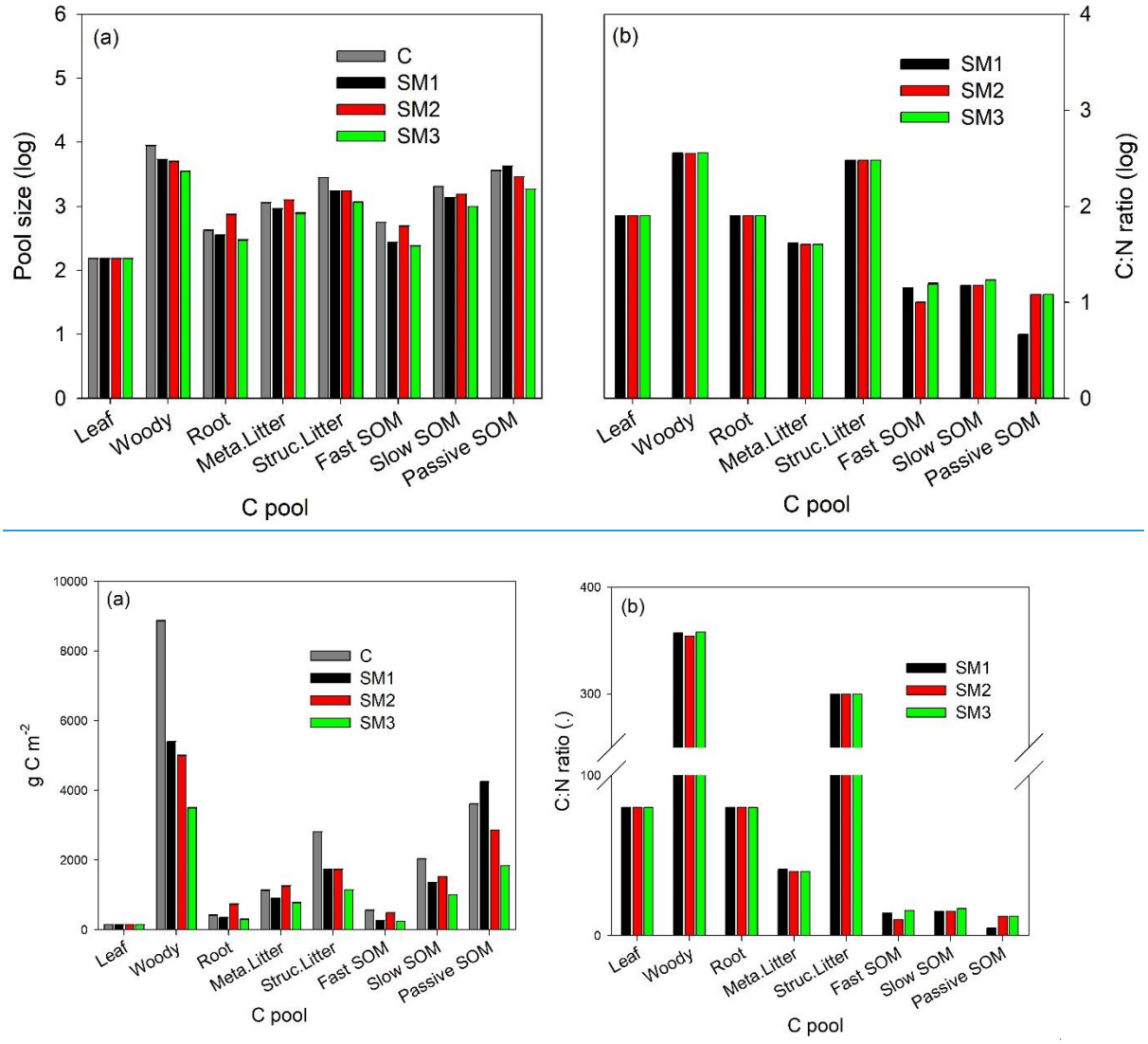

Figure 5. The annual average sizes of carbon pools (panel a) at the steady state among 1996-2007 for C-only version and the three C-N schemes (SM1, SM2 and SM3) and the C:N ratio (panel b) of each carbon pools for the three C-N schemes (SM1, SM2 and SM3) in TECO-CN model.

Figure 6

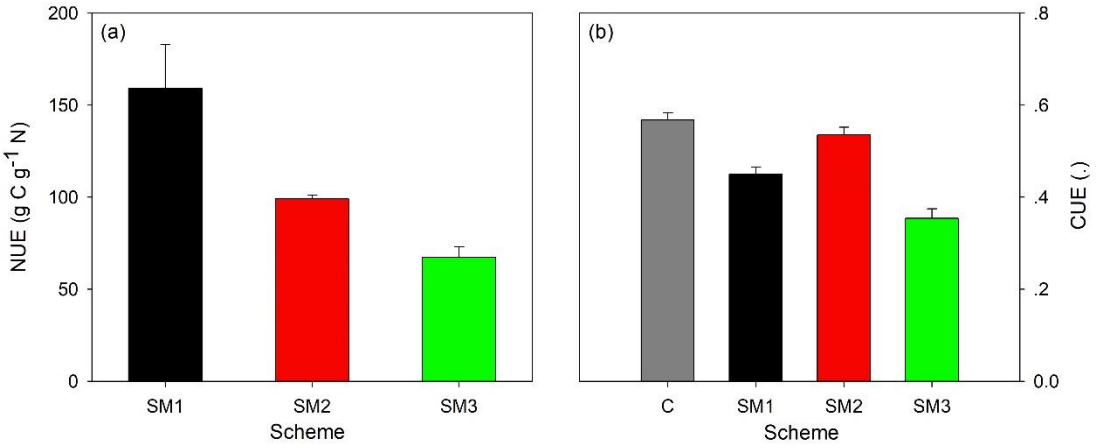

Figure 6. The nitrogen use efficiency (NUE, the ratio of NPP:PNU, panel a) in three C-N schemes of TECO model (SM1, SM2 and SM3) and the carbon use efficiency (CUE, the ratio of NPP:GPP, panel b) at the steady-state among C-only version and the three C-N schemes of TECO model (SM1, SM2 and SM3).

Figure 7

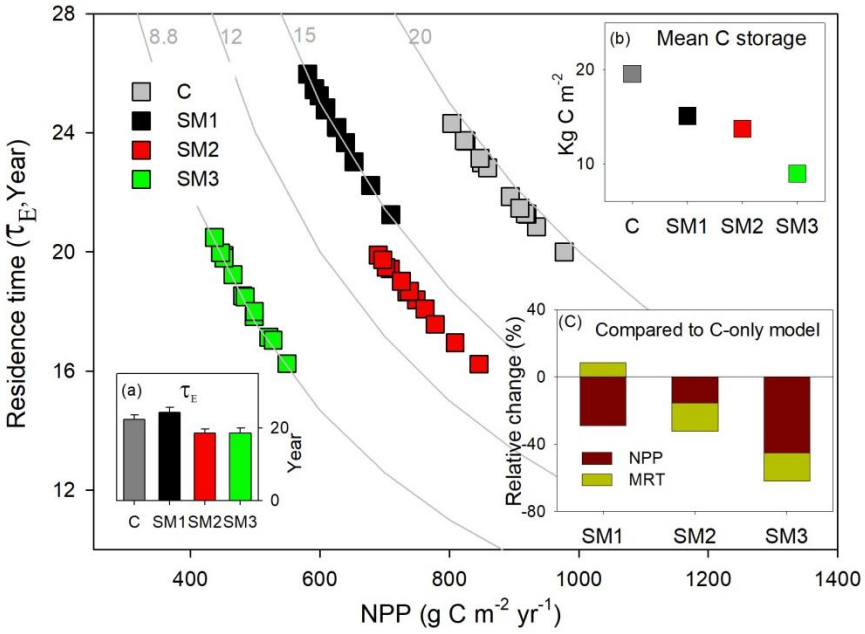

Figure 7. Simulation of annual ecosystem carbon storage capacity for 1996 to 2006 at Duke Forest by carbon in flux (NPP, x axis) and ecosystem residence time (τ_E, y axis) in TECO model framework with three carbon-nitrogen coupling schemes (SM1, SM2 and SM3) and in TECO C-only model (C). The hyperbolic curves represent constant values (shown across the curves) of ecosystem carbon storage capacity. Inset (a), ecosystem carbon residence time (τ_E) in SM1, SM2, SM3 and C-only model; inset (b), mean ecosystem carbon storage simulated among SM1, SM2, SM3 and C-only model; inset (c), relative change of NPP and ecosystem residence time simulated among three schemes compared with in C-only model.

Figure 8

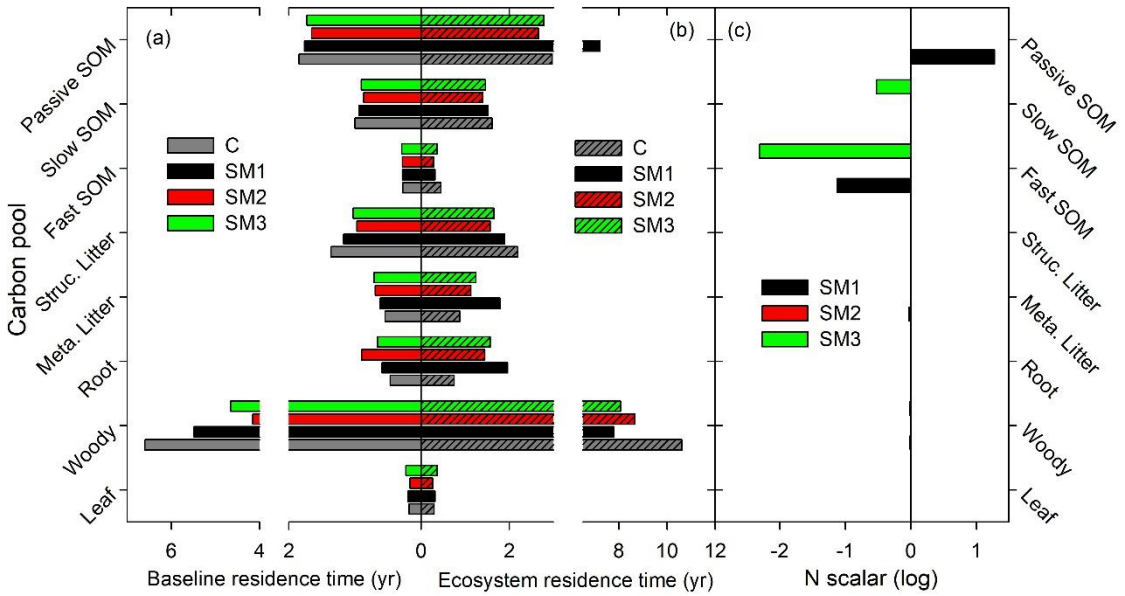

Figure 8. Determination of carbon-pool residence times based on traceability analysis framework in TECO C-N model with three C-N coupling schemes (SM1, SM2 and SM3) and TECO C-only model (C). Panel (a), baseline residence time; panel (b), mean residence time, and panel (c), nitrogen scalar.

Figure 9

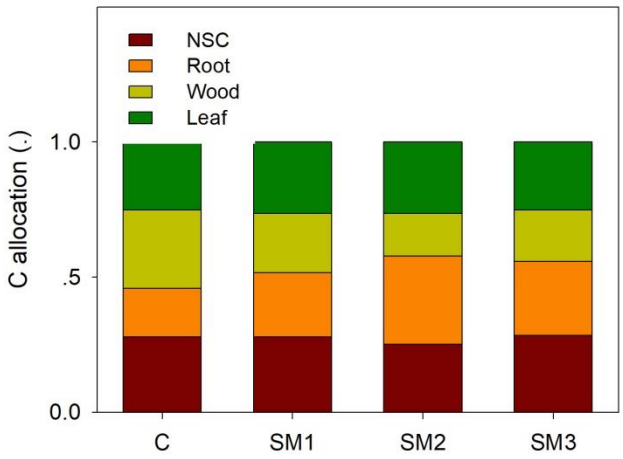

Figure 9. Coefficients of partitioning of NPP to nonstructural C (NSC), root, woody and leaf in C-only model (C) and C-N coupling model with three schemes (SM1, SM2 and SM3).

Figure 10

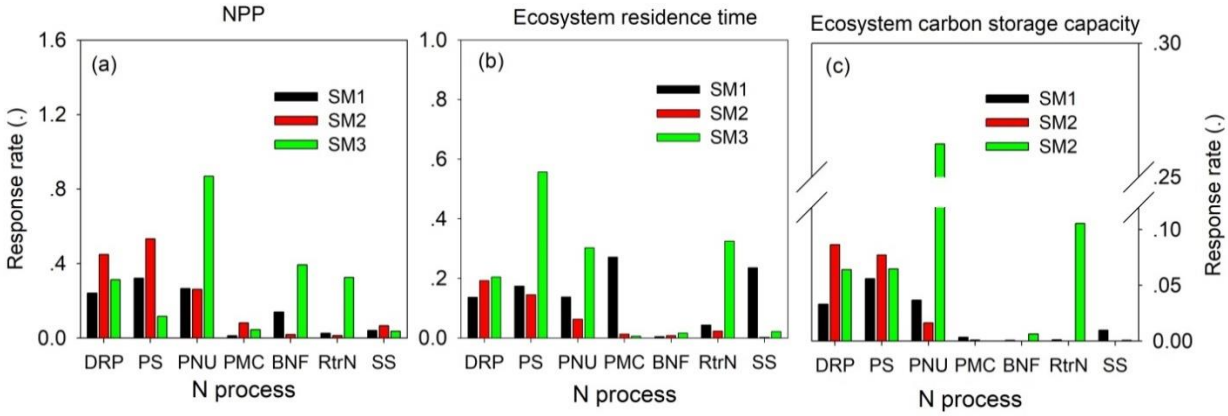

Figure 10. The sensitivity of nitrogen processes to NPP (panel a), ecosystem residence time (τ_E, panel b), and ecosystem C storage capacity (panel c) among three carbon-nitrogen coupling schemes (SM1, SM2 and SM3). DRP, down-regulation of photosynthesis; PS, plant tissue C:N ratio; PNU, plant N uptake; PMC: plant and microbe competition; BNF, biological N fixation; RtrN, re-tranlocation N; SS, soil pool C:N ratio.